Fire & Fracture Resistant Smartphone Case for First Responders

A Major Qualifying Project submitted to the faculty of

in partial fulfillment of the requirements for the
degree of Bachelor of Science

April 27, 2023

Noah Kantor: Chemical Engineering, Materials Concentration
Jacob Morin: Chemical Engineering and Mechanical Engineering

Project Submitted to:

Professor Ali Rangwala, Department of Fire Protection Engineering
Professor James Urban, Department of Fire Protection Engineering

Abstract

Electronic devices such as phones are incredibly prevalent in the 21st century, and while they are upgraded every year, they continue to be vulnerable to heat. The goal of this project was to test materials that could be used for the development of a fire-resistant phone case that could allow firefighters to use these devices in high heat environments. Several categories of materials were tested, including glasses, fabrics, laminates, and a phase change material. These tests were conducted at both a low and a high heat flux based on literature review as well as NFPA and NIST guidelines for fire service equipment. Tests were conducted using a cone heater in order to assess the viability of these materials at protecting electronics in a high temperature environment.

Acknowledgements

We would like to thank Professors James Urban and Ali Rangwala for their guidance throughout the course of this project. We would like to thank lab manager Fritz Brokaw for his guidance in the use of the equipment necessary for this project. We would like to thank Diane Poirier for her help in the acquisition of the materials necessary to conduct this project. We would like to thank the Chemical Engineering, Mechanical Engineering, and Fire Protection Engineering Departments at WPI for providing funding for this project. Finally, we would like to thank Westex: Milliken and S.I Howard glass for providing materials free of charge for use in this project.

Thank you.

Table of Contents

Problem Statement

In the modern day, electronic devices are almost a necessity for most people. These devices, primarily phones, travel around on one's person wherever they go. However, these devices do not fare well in many environments, including high heat. Firefighters work in environments with low end heat fluxes of approximately 10 kW/m^2 and high heat fluxes of over 80 kW/m^2, so the temperatures that they face can easily be damaging to electronic devices such as cell phones. Apple Inc. for instance states that iPhones should only be used in environments where ambient temperature is between 0°C and 35°C, and they fail at a temperature of 45°C (Apple Support). With this narrow range of operating temperatures, this project seeks to expand the versatility of allowable environments where electronic technology can be used. Both the front of the phone (the screen side) and the back of the phone need to be protected. The goal of this project is to find thermal protection approaches and materials that can be used to make a durable phone case with high thermal resistance to protect smartphones from the high heat flux of a fire environment.

Background

The most common type of fire that firefighters encounter is the compartment fire. These are fires that are in confined spaces, such as rooms. These fires are typically broken down into three stages: pre-flashover, post-flashover, and decay. During the pre-flashover period, also called growth, a layer of hot smoke forms and rises to the top of the room. During this time, the temperature at the bottom of the room is relatively low. As the fire grows, the layer of smoke also grows. This smoke acts as a source of a high radiative heat flux. Good ventilation is essential for the development of the fire, otherwise it will become oxygen starved. Under the right conditions, the growth period ends with flashover. When a compartment fire reaches flashover, the flames rapidly spread leading to a rapid increase in the heat flux and toxic gasses are produced creating deadly conditions.

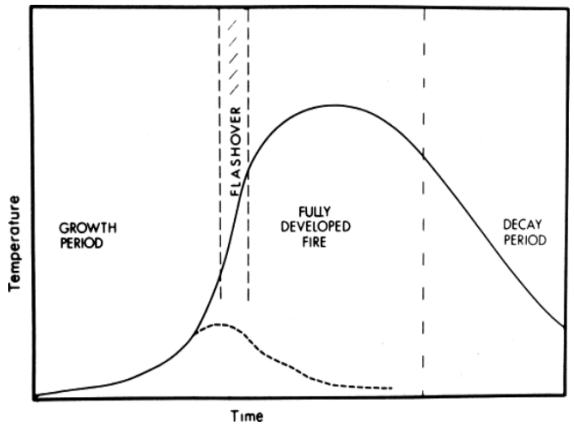

Figure 1: The temperature profile over time of a developing compartment fire. Figure is sourced from "Analysis of the compartment fire parameters influencing the heat flux incident on the structural façade" (Abecassis).

For this project, the focus is on these compartment fires. A firefighter may have their phone or similar device in a position from three feet off the ground to about six feet off the ground. A simple example of a compartment fire environment is given in Figure 2 below.

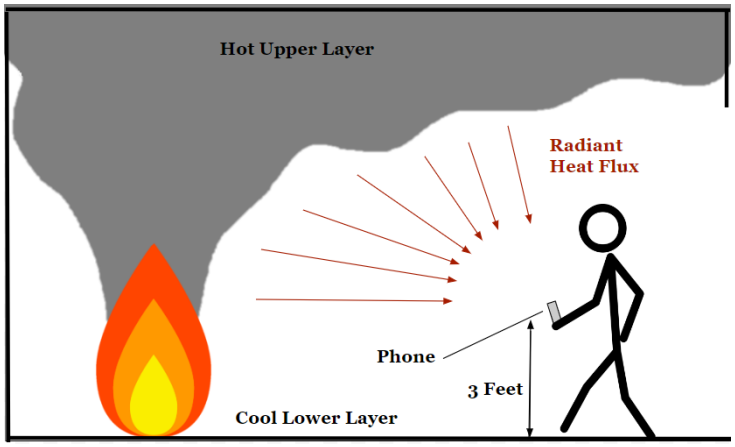

Figure 2: A simple diagram showing the approximate position of a phone in a compartment fire. Heat flux is incoming from both the fire itself and the hot smoke above. The backside and screen of the phone are both exposed to fire when the phone is in use.

Two heat fluxes were tested, a low heat flux representing the general fire environment and a high heat flux representing flashover conditions. The goal is that a phone be usable in low heat flux conditions, and be able to survive high heat flux scenarios. Because of this, crucial aspects like the screen still need to be able to function. This means that in addition to a case, a screen protector should be incorporated into the design.

Theory

When considering this problem of protecting a smartphone from high temperature environments, the first logical step was to analyze exactly what parameters were to be considered. Here we considered four components of the phone and case system. The first is a screen protector to shield the phone screen. The second is the representative device, which is the stand in for the phone. Third is the phase change material (PCM) with thermal pathing, which absorbs heat while melting. Finally, is the laminate layer made from high temperature fabric treated to improve its durability and heat resistant properties. These categories will be further elaborated in the materials and design section of the report.

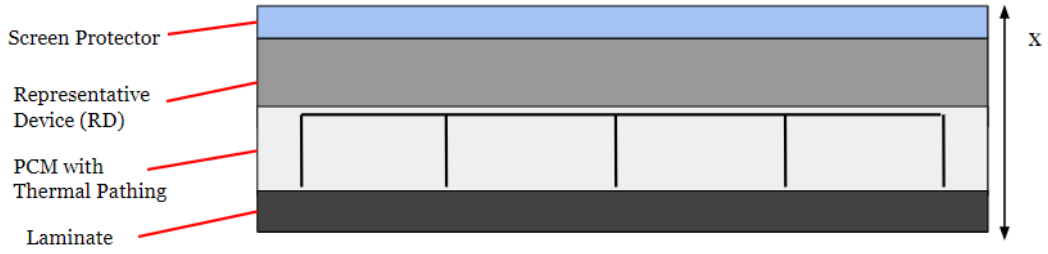

Figure 3: This diagram shows a simplified version of the 1-Dimensional system which will be considered for this analysis. In this investigation, heat flux will be considered along the "*x-direction"* as labeled. This figure is not to scale.

The first boundary condition for the heat diffusion equation that was seen to be the most pertinent was the constant heat flux condition, also known as Fourier's law.

Equation 1: Constant heat flux condition, Fourier's Law (Bergman et. al)

$$-k\frac{\partial T}{\partial x}|_{x=0} = q_s^{"}$$

This equation accounts for radiation that will produce a heat flux towards this device along the *x*-direction. The incident heat flux in this case will come in the form of radiation from the source of heat. Our chosen source of heat for our experimentation will be a cone calorimeter heater. This will be used to simulate the radiative heating of a structure fire. For the sake of this investigation, any heat flux outside the directions labeled in Figure 3 are deemed to be negligible. In combination with this first condition, the transfer of heat through a fluid medium, air, should also be considered.

Equation 2: Convection surface condition (Bergman et. al)

$$-k\frac{\partial T}{\partial x}|_{x=0} = h[T_\infty - T(0,t)]$$

This condition considers the natural convective cooling taking place through our heat testing of materials. The specific apparatus and layout of the testing is explained in greater detail in the Experimental Methods portion of this report.

In addition, radiation will be the source of our heat testing, supplying a constant heat flux on our sample. Heat flux from radiation can be described using the following expression:

Equation 3: Radiation Flux (ignoring re-radiation)

$$-k\left.\frac{\partial T}{\partial x}\right|_{x=0} = \varepsilon F \sigma {T_s}^4$$

Through our examination of our proposed casing system, we test radiative heat flux through both opaque materials and through various transparent glasses. When applying flux directly to these glass substrates, there is a certain amount of reflected as well as transmitted IR radiation. These values are constant at approximately 10% and 90% respectively, as shown by the manufacturers.

When examining real life heat transfer through a substantial volume, there can exist a substantial temperature gradient. This means the temperature is not uniform throughout the object, and therefore would need to be determined. For certain instances, especially physically thin materials with high conductivities and a Fourier number considerably higher than ~0.2, the system can be considered thermally thin, assuming a very small or no thermal gradient. When the system is denoted as thermally thin, transient heat conduction does not need to be considered for calculation, greatly simplifying the problem. Being thermally thin means that much simpler methods of calculation can be used to view thermal behavior over time. The lumped capacitance method is often used in this context. The determination of the system's Fourier number was conducted in Appendix A.

Materials and Design

Representative Device

In place of a phone in our testing, we will use a 2.5in by 2.5in by 0.25in piece of aluminum that will hereby be called the representative device. This is necessary as testing with a real phone would be unsafe and expensive. While the removal of the battery could make a test on a phone less dangerous, the expense of using phones in the testing is still a barrier preventing their use. A heat transfer analysis was performed to verify that aluminum would make an ideal representative device. This analysis assumed that the density of a material multiplied by the heat capacity of that material is approximately equal to $2*10^6$. An iPhone 11 has a volume of $9.482*10^{-5}$ m^3 and a mass of 0.194 kg. With this, the following analysis can be performed.

$$\rho * c \approx 2 * 10^6$$

$$\rho = \frac{0.194\ kg}{9.482 * 10^{-5}\ m^3} = 2046\ \frac{kg}{m^3}$$

$$c \approx \frac{2 * 10^6\ \frac{J}{m^3\ *\ ^oC}}{2046\ \frac{kg}{m^3}} \approx 977\ \frac{J}{kg *^o C}$$

Aluminum 6061 has a heat capacity of 896 J/(kg*^{o}C). These were approximately close enough that the aluminum was determined to be a suitable replacement for a real phone for our testing. There are some flaws in this analysis method, as it assumes a homogeneous material whereas a phone is made up of several different components. In order to justify this analysis, a secondary analysis was performed. This analysis can be found in appendix B.

Initial testing led to some modifications to the representative device. First off, the reflectivity of the aluminum representative device could be causing thermal radiation from the cone to be reflected. To mitigate this, we will use a high temperature spray paint to paint the representative device black. Additionally, applying a thermocouple directly to the top surface of the representative device means that the thermocouple itself will have the heat flux we are testing with applied to it. We drilled a hole into the representative device to get a temperature at the midpoint of the representative device, rather than the front or back surfaces, as this is the ideal point to collect the temperature data.

Screen Protector

The most important component of a smartphone is the screen. This serves as the point from which the user operates with the device. Because the screen is so crucial, there needs to be a way in which the screen can be reasonably protected while still offering the ability for the user to interact with the phone. This means that a screen protector is necessary. This screen protector has a few different necessary characteristics. First, the material chosen needs to be clear, otherwise it would limit the use of the screen. The material also must be thin enough that it will not stop the screen from being used as a touchscreen. The sensitivity of the touchscreen is a function of both the thickness and the permittivity of the screen protector material. Permittivity is the measure by which a material opposes an electric field. As displayed by Figure 4 below, the screen thickness has a much greater effect on the screen sensitivity than the material permittivity.

Because of this, permittivity was not considered as a material property when choosing a screen protector material.

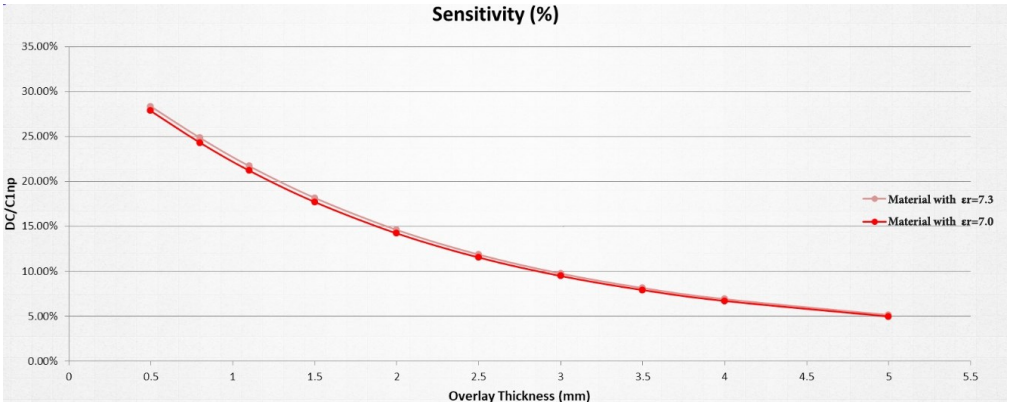

Figure 4: Sensitivity of a touch screen compared to the thickness of the overlay material and the permittivity of the material. The x-axis is the thickness of the material, while the y-axis is the sensitivity of the screen. The two separate lines are tests for two separate materials, with slight differences in their permittivity. Figure is sourced from "Touch Sensor Front Panel: How to Choose the Right Cover Glass" (Fieldscale).

The next need for the screen protector material is thermal resistance. Low thermal conductivity is needed in order to protect the screen from the incoming radiant heat flux and to limit conduction through the screen protector material. The material also needs to be resistant to thermal stresses, otherwise it will be likely to break from extreme heating and cooling.

We performed a test in order to determine the maximum thickness possible for the screen protector that we used. This test was done by purchasing several screen protectors and applying them to an iPhone 11, one on top of the other. These screen protectors were 0.33 mm thick. It was found that applying 3, for a thickness of 1 mm was as thick as we could get with proper screen sensitivity. When a fourth screen protector was applied, the phone screen still worked but was only partially responsive to touch. When a fifth screen protector was applied, there was no response from the touchscreen. Thus, it was determined that a thickness of 1 mm was ideal, with a maximum thickness of 1.33 mm.

Several candidate materials were considered for the screen protector. Based on table 1 below, the Borofloat and the Fused Silica are the most ideal materials for testing as a screen protector material.

Table 1: Ideal screen protector candidate material table. Specifications in this table were determined based on manufacturer marketing (Corning, SCHOTT, Imtera).

Material	Transparent	Ideal thickness	Low thermal conductivity	Thermal shock resistance
Borofloat	Yes	Yes	Yes	Yes
Nextrema	Yes	No	Yes	Yes

Fused Silica	Yes	Yes	Yes	Yes
PYROCERAM	No	No	Yes	Yes
Soda lime glass	Yes	Yes	No	No

Screen Protector Follow-Up Study

A follow-up study was performed to test additional candidate screen protector materials. These included a high temperature quartz glass, as well as several optical filters made by Schott. These optical filters included two neutral density filters (NG5 and NG11), two short pass filters (KG2 and KG5), and an NIR Cut 2 (BG38) filter. The optical filters were chosen as they all had promising internal transmittance, but also had a range of transmittance values to discern the effectiveness of manipulating internal transmittance of the screen protector material. These materials can be seen in the figure below.

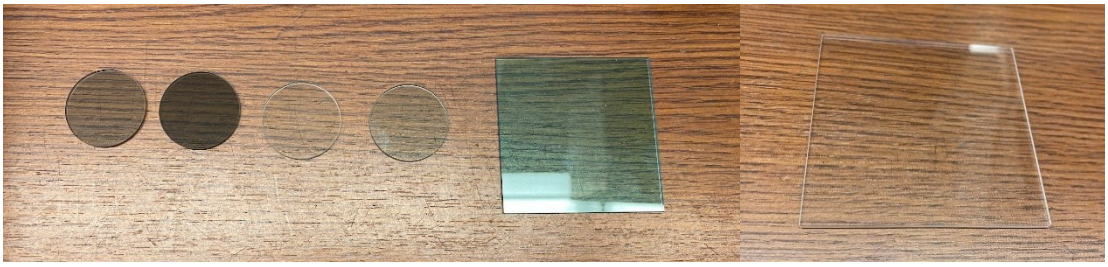

Figure 5: The materials used in the follow-up study. From left to right: NG11, NG5, KG2, KG5, BG38, and Quartz high temperature glass.

The internal transmittance properties of these filters were taken from the material data sheets of these filters (SCHOTT). Based on the internal transmittance data provided by Schott, it can be predicted that the KG5 will be the best performing of the Schott optical filters as it has the least internal transmittance in the IR range. This data is in Figure 6 below. The Planck Black-Body spectrum included in the transmittance figure shows the IR wavelengths produced at the

temperature of 411°C. This is the temperature of the cone heater when producing the 20 kW/m² heat flux.

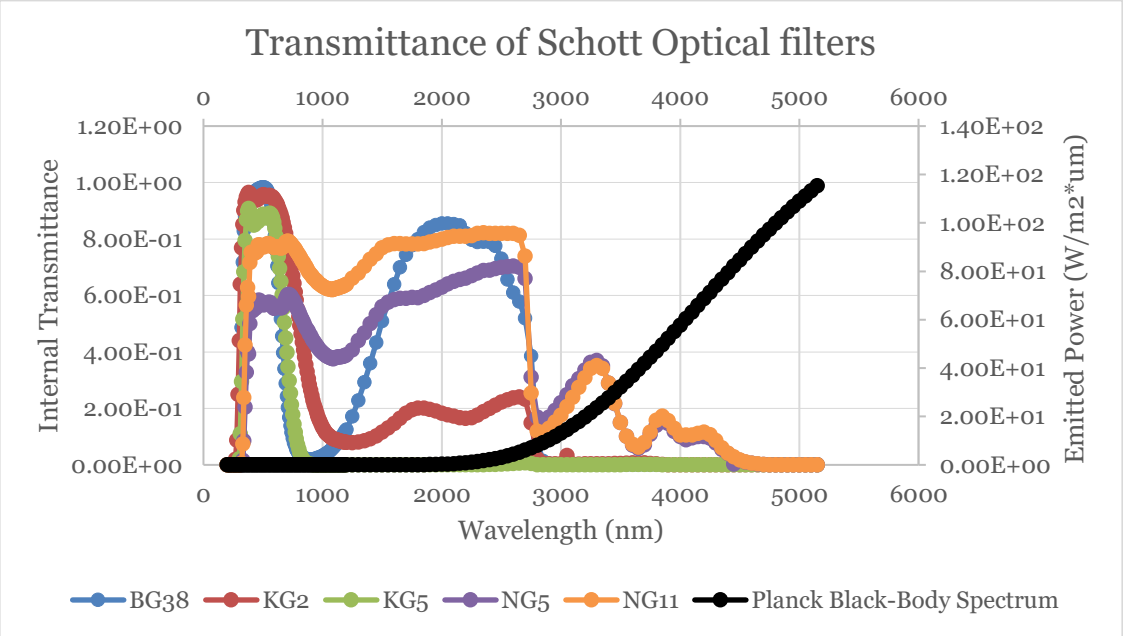

Figure 6: The internal transmittance data for the optical filters tested in the follow-up study performed in D-term. The Planck Black-Body Spectrum is plotted on the secondary axis on the right side of the figure for the temperature of 411°C.

The Schott optical filters were smaller in size than the previous materials tested. Because of this, a new representative device was made for this portion of the project. This representative device was a circle with a diameter a little less than 1 inch and a thickness of 0.25 inches. Rather than drilling a hole into the side of the representative device, a hole was instead drilled into the bottom of the representative device. This hole was 0.125 inches deep, going halfway through the bottom of the representative device, thus the thermocouple probe was 0.125 inches from the surface of the representative device. This hole had a diameter of 0.125 inches. Like with the last representative device, the top surface was painted black to reduce reflectivity. Other than the change in the representative device, experimental conditions remained unchanged.

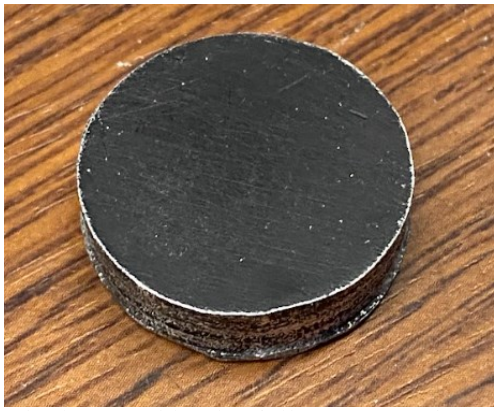

Figure 7: The representative device used in the follow-up study.

Phase Change Material

Phase change materials (PCM's) are one possible method for mitigating the heat transfer into the phone. PCM's are materials selected based primarily on their melting point and heat of fusion so that they absorb a great amount of heat while changing from liquid to solid. For this experiment, the ideal melting point is 35°c, as the PCM needs to melt at a temperature lower than that at which the phone will be destroyed or it will serve no purpose. There are several possible types of PCM's: hydrated salts, metals, paraffin wax, and non-paraffin organics. The relevant properties for these materials can be found in table 2 below.

Table 2: Properties of various types of phase change materials relative to one another. Table sourced from PCM Selection | PCM Technology.

Properties	Paraffin Wax	Non-Paraffin Organics	Hydrated Salts	Metallics
Heat of Fusion	High	High	High	Medium
Thermal Conductivity	Very Low	Low	High	Very High
Melting Point (°c)	-20 to 100+	5 to 120+	0 to 100+	150 to 800+
Latent Heat (kJ/Kg)	200 to 280	90 to 250	60 to 300	25 to 100
Corrosivity	Non-Corrosive	Mildly Corrosive	Corrosive	Sometimes Corrosive
Economics	Inexpensive	Very expensive	Very inexpensive	Expensive
Thermal Cycling	Stable	Decomposes with high temperatures	Unstable over repeated cycling	Stable
Weight	Medium	Medium	Light	Heavy

Non-paraffin organics were not an option considered in this project as they were too expensive for the budget, and thus were unavailable for use in this project. Metals are also not an option for this project, as their high melting points make them useless as a PCM in this endeavor, since the phone would be destroyed before the melting of the metals began (PCM Selection | PCM Technology).

The next option considered was hydrated salts. Hydrated salts have some properties that make them viable for this project. They are inexpensive, have a high heat of fusion, and are light. Additionally, there are several hydrated salts with ideal melting points for the application that we

need. They generally have a high thermal conductivity, meaning that the heat would be spread through the PCM and it would all melt. However, they are mildly corrosive and become unstable with constant thermal cycling. The corrosivity of the hydrated salts would limit the other materials that can be used with them, and over time require the replacement of these materials. Hydrated salts are used extensively as a phase change material for storage of thermochemical energy in low temperature environments. Ultimately, while hydrated salts have many ideal properties for use as a phase change material, they were passed over for consideration in this project as there was not enough support in the literature for their use in high temperature environments (Dixit et al.). In the future, the viability of hydrated salts for this application should be tested, however this testing falls out of the scope of this project.

This leaves paraffin wax, which was determined to be the PCM we would use for this project. Paraffin wax is suitable due to its high heat of fusion and suitable melting point. They are also able to be thermally cycled reliably, are not corrosive, and are not too heavy. Though they cost more than hydrated salts, they are still inexpensive. There are a few pitfalls of paraffin wax that must be considered. The first of these is the low thermal conductivity. This means that thermal pathing of some kind will be required in order to apply heat to the entirety of the phase change material rather than just the external layer. Additionally, there is a volume change associated with the melting of paraffin wax, so additional space will be required in the system to account for this volume change. The primary problem with paraffin wax is that it is combustible. Paraffin wax flash points generally lie around 170°c. An additional insulative layer should be used in order to ensure that it is not possible for the PCM to reach that flash point (PCM Selection | PCM Technology). Paraffin wax would not be ideal for a product of this nature due to its combustible nature, however due to the lack of literature support for hydrated salts compared to paraffin wax, we chose the paraffin wax for this project. Should the paraffin PCM prove effective, it will show that phase change materials can be an effective material for this application and enhance the justification to investigate other materials like hydrated salts. The wax that we chose for our design was Rubitherm Technology's RT 35 HC. This material was chosen for its ideal melting point of 35°C and its high heat of fusion of 240 kJ/kg (Rubitherm Technologies).

The thermal pathing that we used was a square of stainless-steel mesh with aluminum fins welded onto it. The mesh square was meant to keep the fins from falling as the PCM melts, as well as channel heat out of the representative device into the PCM while the PCM is in the back orientation. The aluminum fins will distribute heat vertically through the PCM so that it melts more uniformly. The thermal pathing can be seen in Figure 8 below, as well as in Figure 9 with the paraffin wax. Figure 10 shows how heat is distributed by the thermal pathing through the PCM.

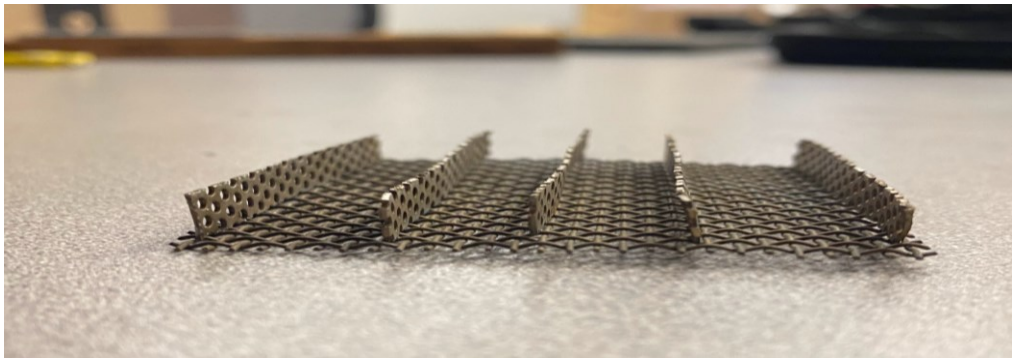

Figure 8: Thermal pathing design for a paraffin wax PCM requiring thermal pathing due to low thermal conductivity in the PCM. The bottom mesh is stainless steel while the fins are aluminum.

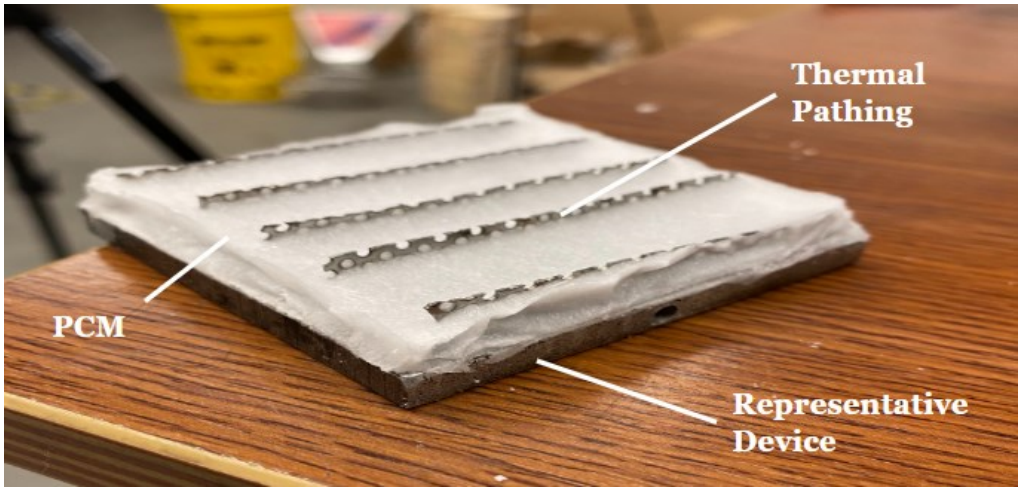

Figure 9: Thermal pathing filled with paraffin wax on top of the representative device.

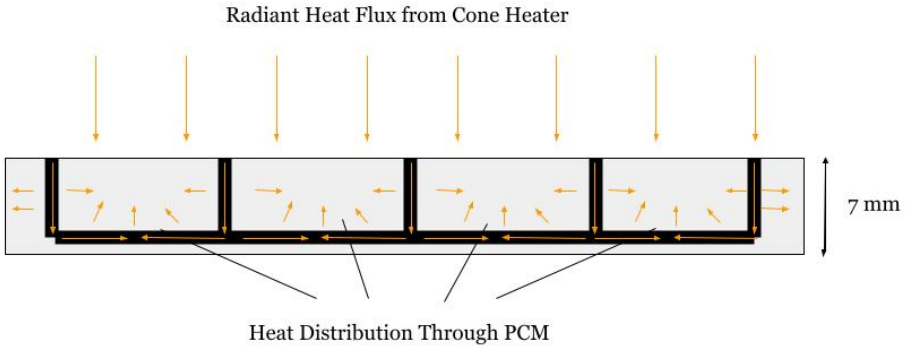

Figure 10: Figure showing how heat is distributed through the PCM with the thermal pathing. Without the thermal pathing, heat is only hitting the top of the PCM layer, and is not distributed by the metal of the thermal pathing.

While we used the thermal pathing that we made, we also considered using heat sinks. Premade heat sinks are more optimized than what we used, but we elected not to purchase one. This is primarily because the thermal pathing we made serves the purposes of the project, and heat sink purchase was not necessary. Additionally, the matter of thermal pathing effectiveness

was deemed beyond the scope of this project. In the future, heat sink effectiveness through PCM should be investigated.

Laminate

While PCM's are a promising option for absorbing heat to protect the phone, they alone would not be sufficient. Another layer is necessary as there needs to be a vessel to contain the PCM once it becomes a liquid, as well as provide an additional insulative layer. Additionally, this casing is necessary to provide structural rigidity if the phone is dropped. While there are many possible materials for the phone casing, many have properties that make them less ideal. Metals are durable and machinable, but they also have high thermal conductivity values. This makes metals a subpar material for the casing design. Thermoplastics are durable and have high heat resistance, but their high cost means that they are too expensive to be an option for this project, and melting is possible at very high temperatures. Many ceramics have both the durability and thermal resistance necessary for our material needs, however ceramics are generally not machinable. This means they are not an ideal candidate as the non-machinable aspect means that it would be expensive to produce the casing and hard to work with. An alternative to these traditional materials is a laminate. A laminate can be made with some form of heat resistant fibers and adhesive. A laminate would be feasible to fabricate and it would become rigid once it cures.

Initially, Nomex was the material considered for making the laminate. Nomex is the fibers used to make the fabric for firefighter turnout gear. It is highly heat resistant, and when combined with an adhesive it could form a laminate that would be easy to fabricate and would be extremely rigid (Barker et. al). Specifically, this fabric is used in a knit pattern covering various parts of the firefighter's body, including the head, hands, and torso to act as a heat shielding. However, there is very little literature regarding the use of Nomex as a material for making a laminate, and what did exist was not based on heat resistant properties of the laminate. Because of this, we also investigated fiberglass fibers for the laminate. The use of fiberglass laminates to make heat resistant materials is well established in literature. Notably, the concept of heat resistant fiberglass lamination was documented from NASA's Gemini space program. In NASA's investigation prior to the Apollo Missions, test crafts were fitted with heat shielding constructed of resin impregnated fiberglass acting as a laminate (Venkatapathy). A potential manufacturer of the fiberglass that could be used for making the laminate is Auburn Manufacturing. Located in Auburn, Maine, they manufacture a wide variety of fiberglass materials specifically engineered for heat resistance in very high temperature environments (Auburn Manufacturing).

The adhesive for the laminate construction has two primary requirements. The first is that the laminate made with this adhesive must be rigid and strong. This means the outer casing fabric can be molded into a desired shape and cured to form an inflexible structure. The second is that it must be able to withstand very high temperatures. This is where organic adhesives fail, as the high temperatures that are needed for this design cause organic adhesives to break down. Multiple adhesives were considered for this project. The first was the Accumet Refractobond ALS. The second was the Aremco PyroPaint 634-AS1. Both materials are inorganic ceramic adhesives with a high temperature range. They are chemically resistant and are suitable for a strong, rigid

laminate. Ultimately, the Aremco PyroPaint 634-AS1 over the Accumet Refractobond ALS due to pricing. The two laminates that were made are in the figure below.

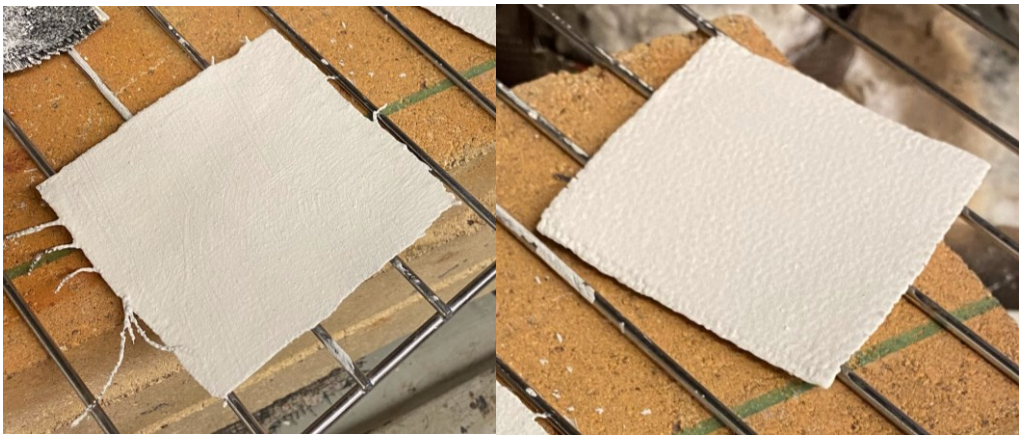

Figure 11: The Nomex laminate (left) and the AS fiberglass laminate (right) prior to testing.

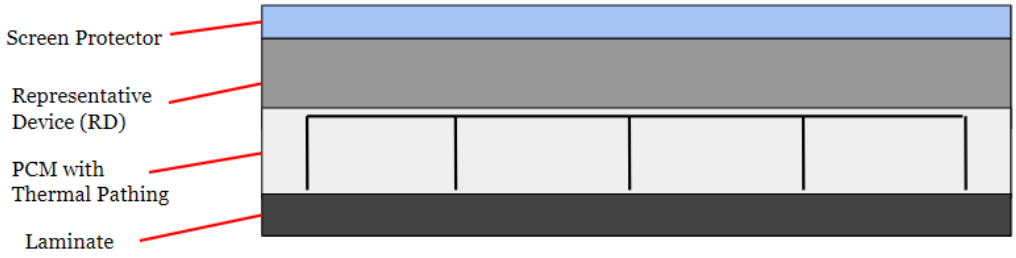

Figure 12: General design for the full casing layout. From back to front (bottom to top in this figure), the layout consists of the laminated outer casing, the PCM with thermal pathing, the representative device, and the screen protection glass. This figure is not to scale.

Experimental Methods

The planned testing apparatus uses the cone heater from a cone calorimeter to apply heat flux to the testing specimen. The cone heater was chosen because it is available to us, easy to control the heat flux to the specimen, and it provides a spatially uniform heat flux. This apparatus is designed to be used to test one dimensional heat transfer into the specimen. This is done by insulating all but one side of the testing specimen so that only the desired testing surface is exposed to the heat flux. Similar testing mechanisms have been reported in literature to define the impact of heat flux on the measured temperature of a sample.

Several different experimental testing scenarios were considered when planning this specific apparatus. One experiment was done to test the effectiveness of intumescent (fire resistant) coatings. In this experiment, steel plates were coated with the intumescent layer and exposed to various heat fluxes simulating a structure fire (Bartholmai et al.). Type K thermocouples were used in this experiment. Type K thermocouples are optimal for their ability to handle high temperatures. Type K thermocouples are already available in abundance in the fire protection lab, so we did not need to purchase these.

The thermocouple was able to be placed within the representative device via a ⅛ inch hole made with a drill press. The thermocouple was positioned such that it touched the top face of the drilled hole during testing. This design can be seen below.

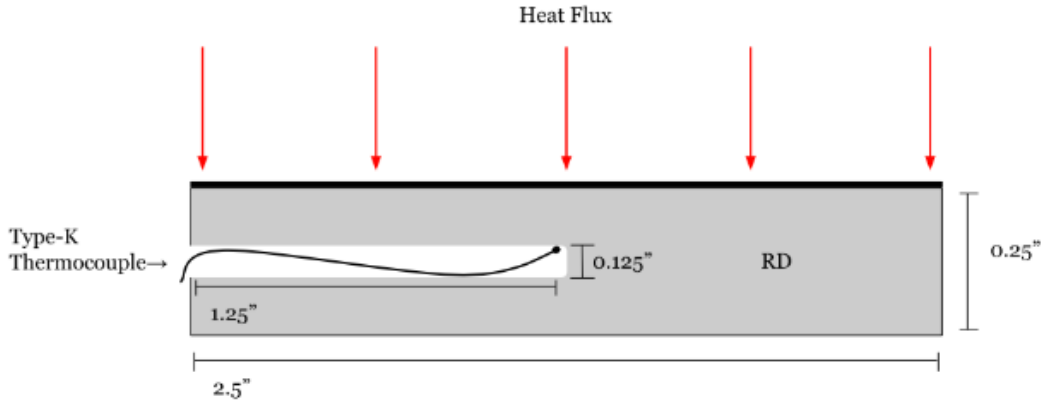

Figure 13: Thermocouple orientation within the representative device. Dimensions provided are accurate, but the figure is not to scale.

The insulation used to insulate the sides of the specimen during testing will be KAO board. KAO board is a strong insulator designed for very high temperatures that can easily be cut as needed. This material is also available in abundance in the FPE lab, so we did not need to purchase this. There are several scenarios that must be tested, a range of fluxes to simulate a standard fire environment exposure, and flashover. Flashover is when extreme heat causes a rapid spread of fire, resulting in a short but extreme heat flux. These tests are designed to replicate both the typical conditions that firefighters face in their everyday work, and to replicate flashovers. These parameters will be defined in the Experimental Conditions.

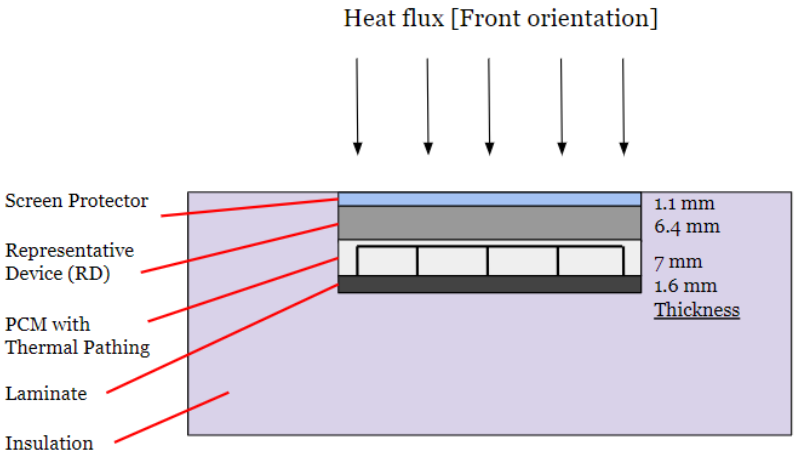

Figure 14: This diagram shows an example of a sample setup which will be tested in our experiments. In this layout, the configuration shows the flux directed at the frontside of the casing system, wherein the "screen" faces upwards towards the heat source. This figure is not made to scale. Additionally, it specifies a laminate thickness of 1.6 mm, but two different laminates were tested, one with thickness of 1.6 mm and one with thickness of 1.5 mm.

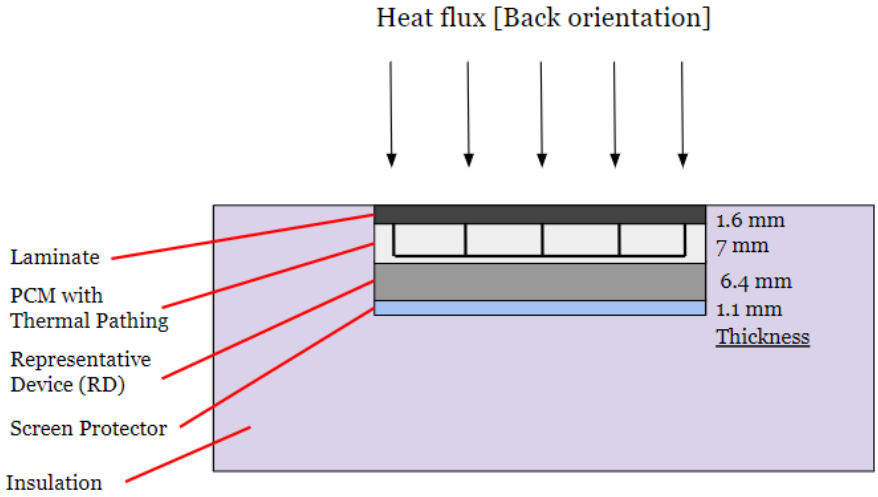

Figure 15: This diagram shows an example of a sample setup which will be tested in our experiments. In this layout, the configuration shows the flux directed at the backside of the casing system, wherein the "screen" faces downwards, away from the heat source. This figure is not made to scale. Additionally, it specifies a laminate thickness of 1.6 mm, but two different laminates were tested, one with thickness of 1.6 mm and one with thickness of 1.5 mm.

Identifying Material Matrix

There are a wide variety of tests that need to be performed. These can be found in table 3, the testing matrix for this project, below.

Table 3: Part 1 on the testing matrix. This table defines how each test will be performed with regards to which materials will be used. The direction at which the heat flux will be entering the system is labeled in brackets. When the screen side is up, that is considered the front configuration.

Material combination tested	ID
Representative device (RD) with no casing	1
RD with borosilicate glass [Front]	2
RD with soda lime glass [Front]	3
RD with unlaminated AS fiberglass fabric [Back]	4
RD with unlaminated GL fiberglass fabric [Back]	5
RD with unlaminated Nomex [Back]	6
RD with laminated AS fiberglass [Back]	7
RD with laminated Nomex [Back]	8
RD with PCM [Front]	9
RD with PCM [Back]	10
RD with Borofloat and PCM [Front]	11
RD with AS laminate and PCM [Back]	12

Experimental Conditions

There are two heat flux scenarios that we will be testing for each of the materials combinations. These are a low heat flux and a high heat flux, found in table 4 below.

Table 4: Part 2 of the test matrix, this displays the flux that will be applied to the testing sample and over what amount of time that flux will be applied (Foster, NIST, NFPA).

Flux ($\frac{kW}{m^2}$)	20	70
Time (s)	60, or until internal temperature of RD reaches 45℃	30, or until internal temperature of RD reaches 45℃

With each of these trials, temperature vs. time data will be recorded between each component using type K thermocouples. This will allow for a proper examination of the thermal insulating properties of the individual layers. These conditions were obtained by cross-referencing various pieces of literature and through NIST and NFPA guidelines.

In NIST Technical note 1474: Thermal Environment for Electronic Equipment Used by First Responders, several records of tests are outlined both for personal firefighting gear and exposure limits which firefighters can withstand (NIST). For example, in this note, it was cited that firefighters were only able to withstand radiant heat fluxes of 10 kW/m^2 for 1 minute (NIST, Foster et. al). This means that any device carried with the first responder should also be able to withstand this duration under the same or higher flux. Although the cone calorimeter heater cannot provide this low of a flux stably, it can give consistent flux at 20 kW/m^2 so this flux was used instead. Notably, this means that our tests are performed under harsher conditions than the standard. In the same technical note by NIST, NFPA 1971 was referenced in regards to the testing done on protective garments such as gloves and multilayer protective gear. These tests require a flux of 83 kW/m^2 for a duration of 30 seconds (NIST, NFPA). Since, again, the cone calorimeter heater cannot provide consistent flux this high, we tested at 70 kW/m^2 for a duration of 30 seconds. These tests should provide both higher end exposure limits as well as extreme conditions which firefighters and their gear would experience.

Under a low heat flux such as 5 kW/m^2, a firefighter could use their phone, though this heat flux would not be comfortable. At a heat flux of 20 kW/m^2, a firefighter might check their phone or similar device, but would be unlikely to use it for any extended period. At a heat flux of 70 kW/m^2, a firefighter would secure their phone and get out as soon as possible. The goal is that the phone be usable at low heat fluxes, and be able to survive at high heat fluxes.

Results and Analysis

Heat Transfer Modeling

The heat transfer of this system is transient in nature, meaning typical steady state analysis methods do not work for this application. We are interested in several aspects of the phone casing system, but our main concern is the internal temperature of the phone. In addition, the PCM should also be considered as it undergoes a phase change from solid to liquid, absorbing large amounts of heat as it does so.

In order to create a much simpler system to analyze, the lumped capacitance method was used. These calculations were concentrated on the PCM, using 3 separate temperature intervals to see what time it took to reach each given interval. The three intervals went as follows:

t_1: time to reach 35℃ (the melting point of the PCM)
t_{melt}: time to fully melt PCM
t_2: time to exceed 45℃ following the melt

It should be noted that 45℃ was arbitrarily chosen as a temperature much higher than that of the melting. For this analysis, an energy balance was used to establish the basis for the time interval calculations on just the phone. This can be shown as the following:

$$E_{sys} = \Sigma q_{in} - \Sigma q_{out} + E_{gen}$$

Where the energy of the system should equal the heat going in subtracted by the heat going out. In the absence of any chemical reactions, the $E_{gen} = 0$. Using this energy balance, the following relationship was formed:

$$\rho A_s \Delta x \frac{dT}{dt} = (q''_{ext} A_s) - hA_s(T - T_\infty)$$

With ρ as density, Δx as thickness, A_s as the surface area, and q''_{ext} representing the outside radiant heat flux from the cone heater. Through integration, this can be solved to achieve the following:

$$ln\left(\frac{T(t_1) - T_\infty - q''_{ext}/h}{T(0) - T_\infty - q''_{ext}/h}\right) = \frac{-ht_1}{\rho C \Delta x}$$

For a given time, t_1, the expression can be rearranged into the following, where the $\rho C \Delta x$ term is divided into the constituent parts of the phone casing system:

$$t1 = \frac{(\rho_{Fib} C_{Fib} \Delta x_{Fib} + \rho_{PCM} C_{PCM} \Delta x_{PCM} + \rho_{Glass} C_{Glass} \Delta x_{Glass} + \rho_{Phone} C_{Phone} \Delta x_{Phone})}{-h} ln(\frac{(T(t1) - T_\infty - q''_{ext}/h)}{(T(0) - T_\infty - q''_{ext}/h)})$$

Table 6: Parameters used in calculation of melting time. It should be noted that many values were taken directly from the manufacturer, which is the case with the Borosilicate (SCHOTT) and the PCM (Rubitherm Technologies). For the Laminate, data was limited, so general data on fiber glasses were used (Architectural Fiberglass). For the phone, properties of aluminum were used (Engineering Toolbox).

Property	Glass	Phone	PCM	Fiberglass Laminate

ρ (kg/m^3)	2200	2700	880	2500
$C\ (J/\ kg\ K)$	830	900	2000	790
$\Delta x\ (m)$	0.0011	0.00635	0.01	0.00368
$A_s\ (m^2)$	0.00403	0.00403	0.00403	0.00403
$V\ (m^3)$	0.00000443	0.00002559	0.0000403	0.00001483
$m\ (kg)$	0.0097526	0.06909435	0.035464	0.037076

Table 7: PCM properties and heat transfer conditions (Rubitherm Technologies).

Property	Value
$\Delta H_{fusion}\ (J/kg)$	240000
$T_{melting}\ (K)$	308
$T_\infty\ (K)$	295
$q''_{ext}\ (W/m^2)$	20000
$h\ (W/m^2\ K)$	15

For $t(0)$ to t_1 Equation 1 was used to find the total time taken to heat the PCM from ambient temperature to the melting point of the PCM. Under the conditions listed previously, $t_1 = 27.6\ seconds$

Applying an energy balance to control volume around the PCM:

$$E_{in} = \Delta E_{st} = \Delta U_{lat}$$

By examining natural convection and an influx of radiant energy, the following expression can be made about the system:

$$t_{melt} = \frac{\Delta H_{fus}\rho\Delta x}{-h(T_{melt}-T_\infty)+q''_{rad}} \quad (2)$$

Using all the properties from Table 7, and the density and thickness of the PCM from Table 6, it was found that $t_{melt} = 107\ seconds$

With Equation 1 once more, the time taken following the melting of the PCM was examined. This interval t_2 was set to end at 318 K, where a typical phone breaks from overheating. It was determined that interval $t_2 = 21.4\ seconds$. Adding all three intervals of time from a temperature of 295 K to 318 K, $t_{total} = 156\ seconds$. These predictions will be discussed and compared with the cone heater tests.

Cone Heater Testing

Testing was done with a cone calorimeter heater in the gateway fire protection engineering lab. The cone that we are using has aged, and because of this some constraints had to be put on the experimental conditions due to the device's operability. Initially, the lower threshold for testing was going to be 10 kW/m² while the upper bound for modeling flashover was going to be 80 kW/m². However, the cone that we are using is only able to achieve a high heat flux of 70 kW/m² and a low heat flux of 20 kW/m². Beyond these conditions, the cone heater is unable to provide a reliable heat flux. For all tests, the thermocouple was positioned in a hole drilled into the representative device, as shown in Figure 13 in the experimental methods section.

Bare RD, 20 kW/m²

The first test performed was the bare representative device test at the 20 kW/m² heat flux. With nothing protecting the representative device, this is the benchmark of comparison for all the following tests performed at the 20 kW/m² heat flux. Additionally, it is included in the figures for all the 20 kW/m² tests in order to provide a direct comparison when looking at each figure. Figure 16 shows the testing set up used when conducting this test. The data from this test can be seen in Figure 17.

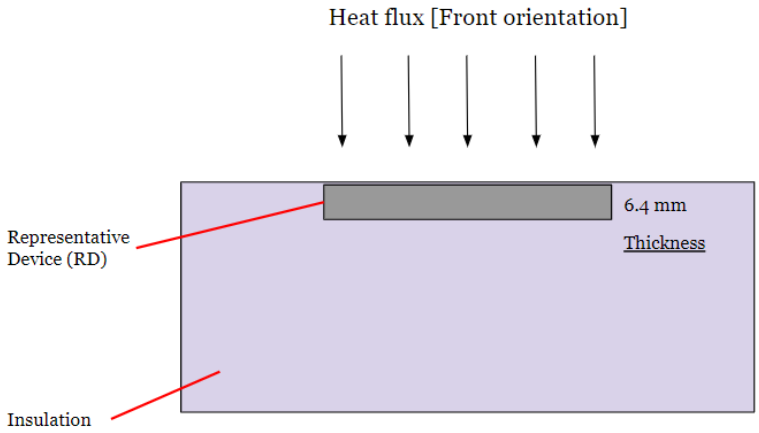

Figure 16: The testing setup used for the bare representative device test. This figure is not made to scale.

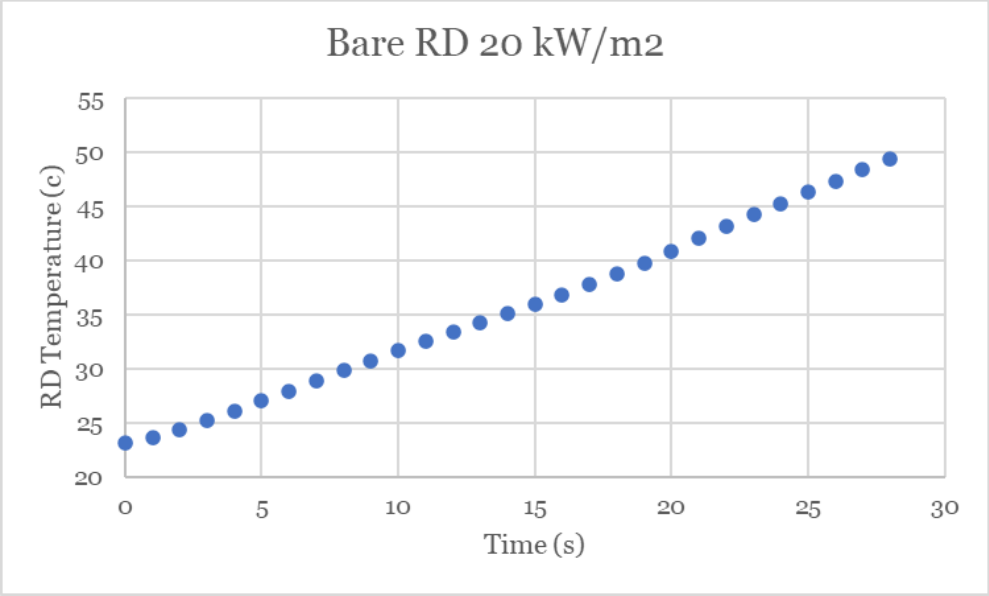

Figure 17: This is the data for the representative device temperature vs time without any measures being used to protect it from the heat flux at 20 kW/m^2.

It can be seen from this figure that it took approximately 14 seconds for the unprotected representative device to reach a temperature of 35^{o}C and approximately 24 seconds to reach 45^{o}C.

Glass Screen Protectors, 20 kW/m^2

The next test performed was using the first glass material, the Borofloat glass. Both glass tests were performed with the setup shown in Figure 18 below.

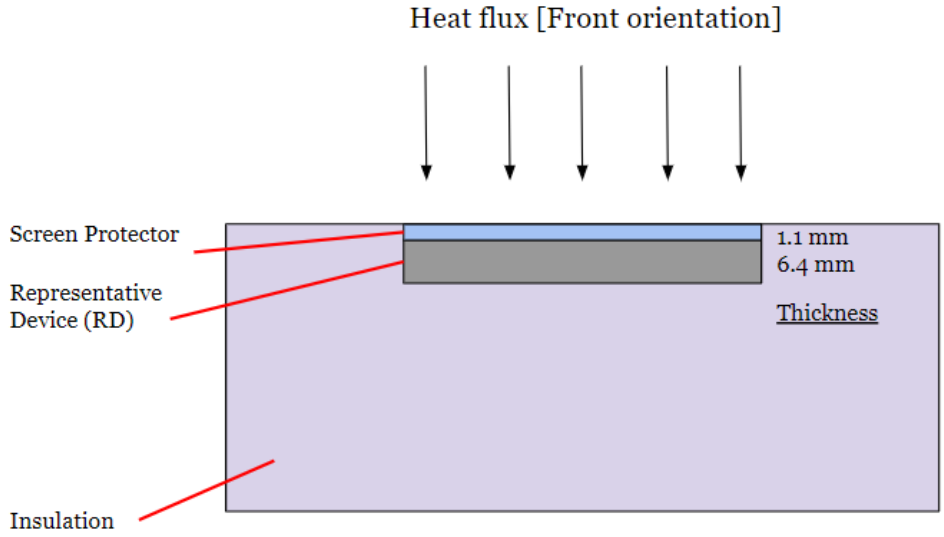

Figure 18: The orientation of the setup used for both the Borofloat and the soda lime glass tests. This figure is not made to scale.

The Borofloat test was performed in the front orientation, wherein the screen would be face up, and the thickness of the glass was 1.1mm. The results of this test are shown in Figure 19 below.

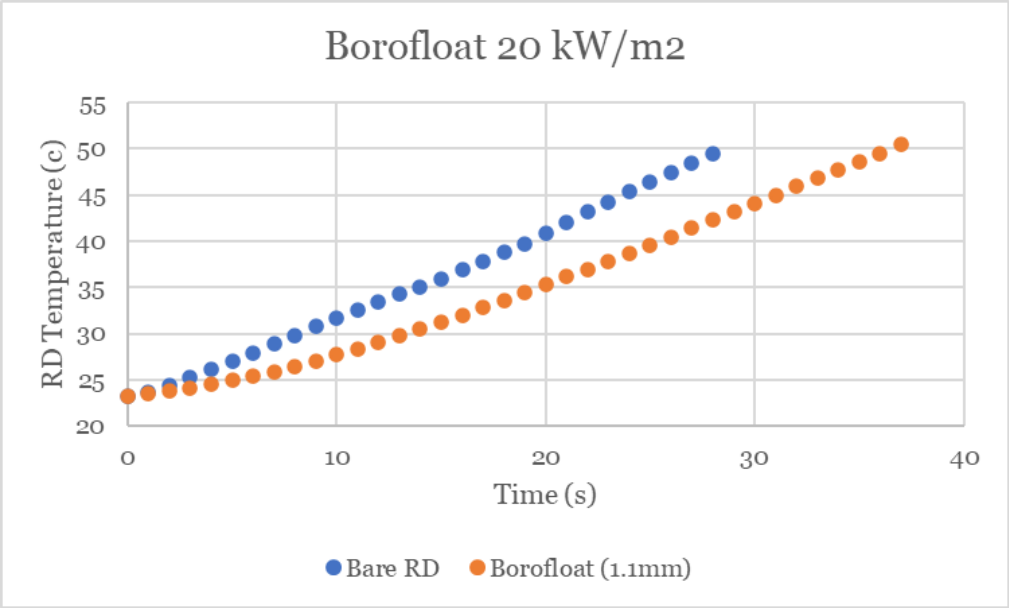

Figure 19: This is the data for the representative device temperature vs time with the Borofloat glass on top of the representative device to shield it from the heat flux at 20 kW/m^2.

The Borofloat glass marginally outperformed the bare representative device, having taken approximately 20 seconds for the representative device to reach 35^{o}C and approximately 31 seconds to reach 45^{o}C.

Following the Borofloat test, a test with the ordinary soda lime glass was performed. As with the Borofloat, the test was performed in the front orientation, and the soda lime glass also had a thickness of 1.1mm. The results of this test are in Figure 20.

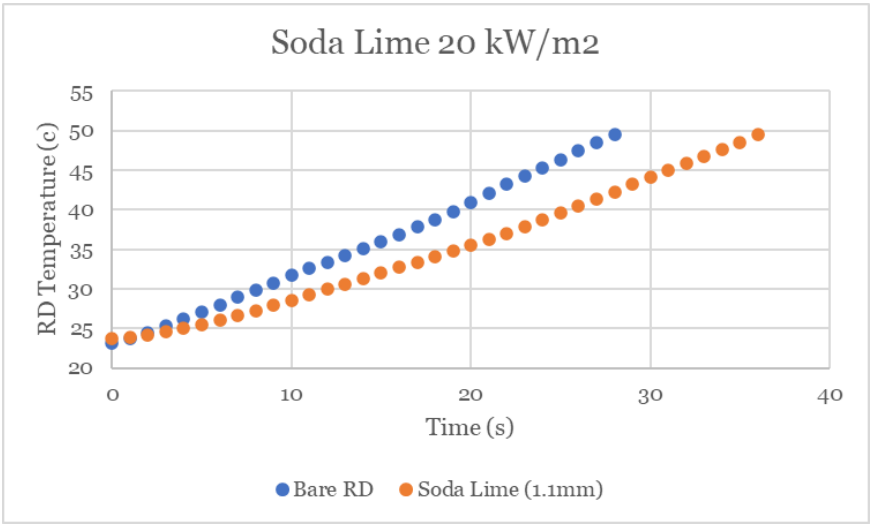

Figure 20: This is the data for the representative device temperature vs time with the soda lime glass on top of the representative device to shield it from the heat flux at 20 kW/m^2.

It took approximately 20 seconds for the representative device to reach 35°C and approximately 31 seconds to reach 45°C.

Fabrics, 20 kW/m²

The next set of materials that we tested was several fabrics. These fabrics were not fully considered as a suitable material for the phone case; however, we tested them to get a benchmark for comparison with our laminates. The orientation of the fabric tests is included in Figure 21 below.

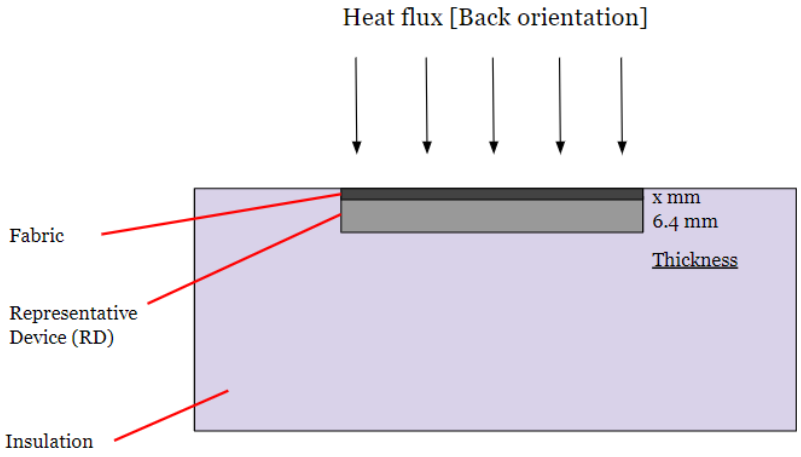

Figure 21: The test setup orientation for the fabric tests. For the Nomex, the thickness, x, is 0.5 mm. For the AS fiberglass, the thickness, x, is 0.85. For the GL fiberglass, x is 0.4 mm. This figure is not made to scale.

The first fabric tested was the Nomex fabric. This fabric has a thickness of 0.5 mm. This test was conducted in the back orientation, wherein the phone screen would be face down and the Nomex fabric would be on top of the representative device, blocking the heat flux from the cone heater. The results of this test are in the figure below.

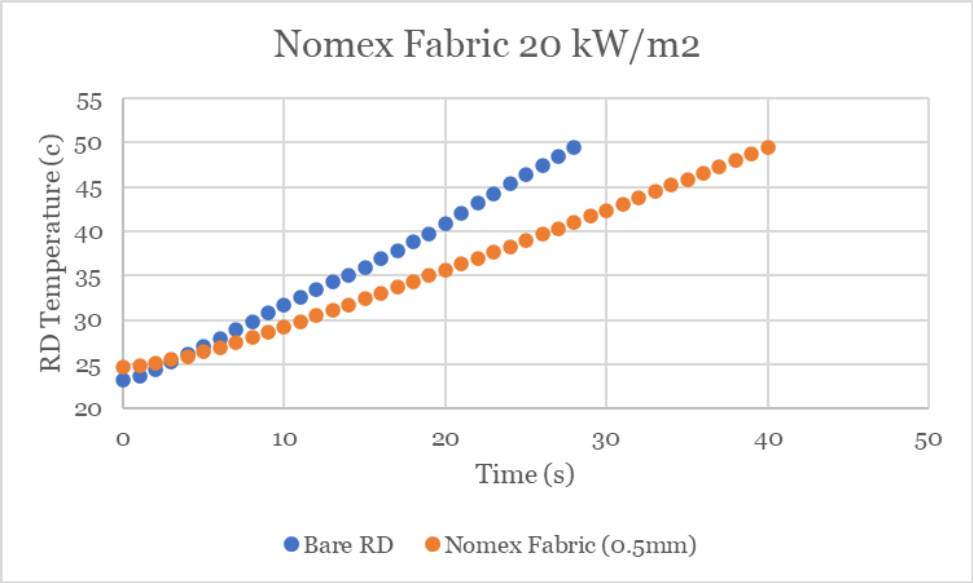

Figure 22: This is the data for the representative device temperature vs time with the Nomex fabric on top of the representative device to shield it from the heat flux at 20 kW/m^2.

It can be seen in this figure that it took approximately 19 seconds for the representative device to reach 35^{o}C and approximately 34 seconds for the representative device to reach 45^{o}C. The Nomex fabric did take damage from this test, with the outside edges of the material being damaged. The before and after photos of the Nomex fabric can be seen below. Neither of the other fabric materials took any damage from the 20 kW/m^2 tests.

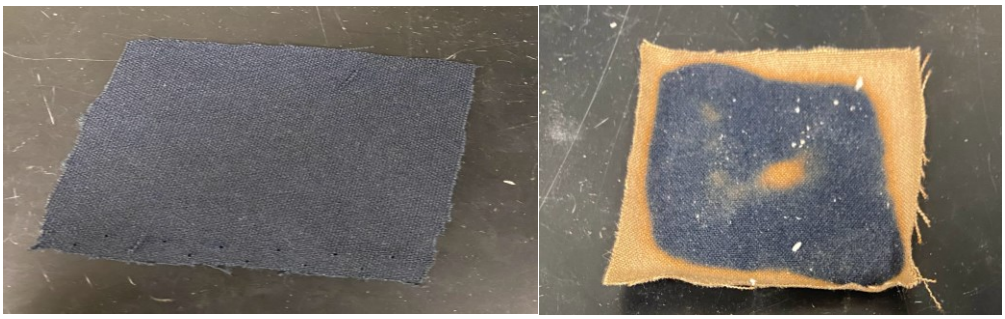

Figure 23: Before (left) and after (right) photos of the Nomex fabric following the test conducted at 20 kW/m^2.

The next test conducted was the AS fiberglass fabric. This fabric was tested in the back orientation in the same manner as the Nomex fabric. It has a thickness of 0.85 mm. The results of this test can be seen in Figure 24 below.

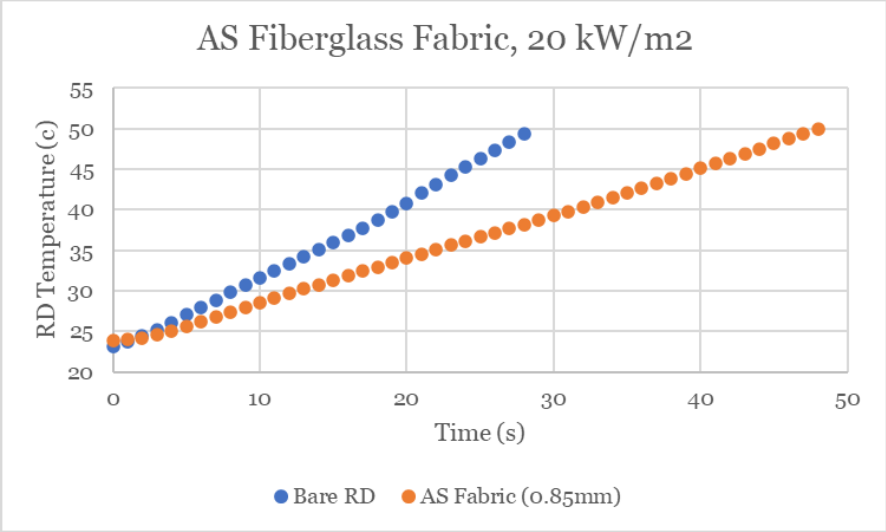

Figure 24: This is the data for the representative device temperature vs time with the AS fiberglass fabric on top of the representative device to shield it from the heat flux at 20 kW/m².

It can be seen from the figure that it took approximately 22 seconds for the representative device temperature to reach 35°C and approximately 40 seconds for the representative device temperature to reach 45°C.

The final fabric tested was the GL fiberglass fabric. This fiberglass was thinner than the AS fiberglass with a thickness of 0.4 mm. As with the other fabrics the test was conducted in the back orientation with the "screen side" down and the heat flux being applied to the fabric on the back side of the representative device. The results of this test are in Figure 25 below.

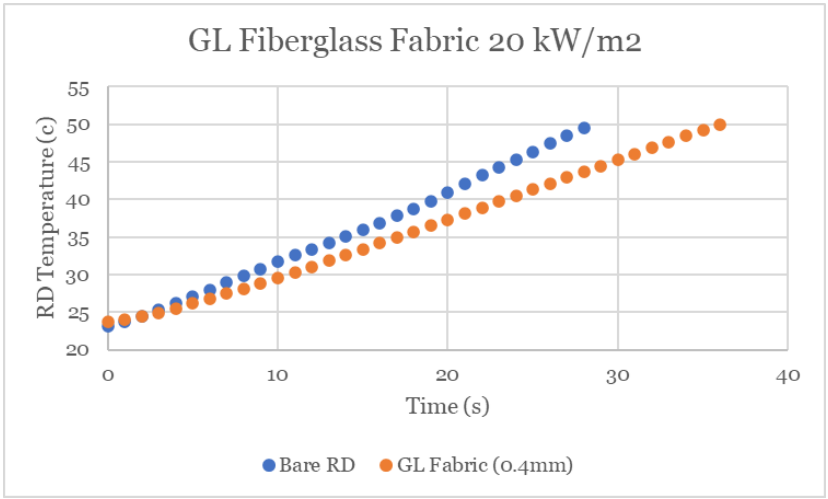

Figure 25: This is the data for the representative device temperature vs time with the GL fiberglass fabric on top of the representative device to shield it from the heat flux at 20 kW/m².

It can be seen from the figure that it took approximately 17 seconds for the representative device to reach 35°C, and it took approximately 30 seconds for it to reach 45°C.

Laminates, 20 kW/m²

Following the testing of the fabrics, we fabricated our laminates and conducted tests using them. Only 2 laminates were made, one with Nomex and one with fiberglass. The AS fiberglass was chosen to be used to make the laminate as it performed better (likely due to both the greater thickness and the lighter color). The orientation for both laminate tests is provided below in Figure 26.

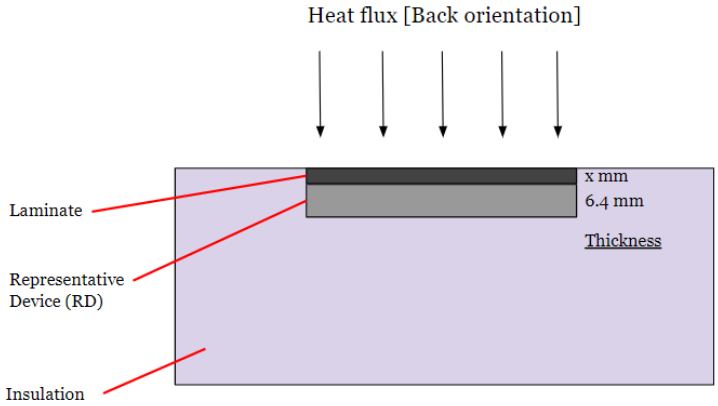

Figure 26: The orientation for the laminate tests. For the Nomex laminate, x is 1.5 mm, while for the AS fiberglass laminate test, x is 1.6mm. This figure is not made to scale.

The Nomex laminate was tested first. It was tested in the back orientation with the screen down and the laminate shielding the back side of the phone from the incoming heat flux. The Nomex laminate had a thickness of 1.5 mm. Figure 27 shows the data collected for this test.

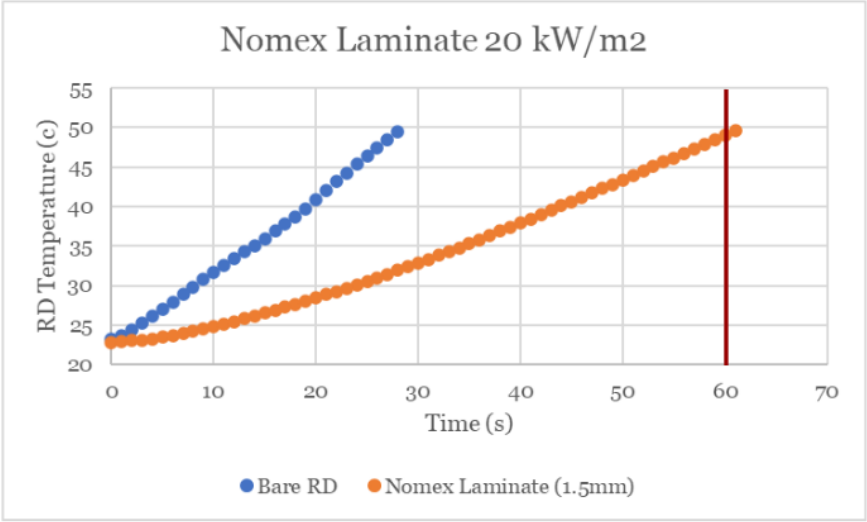

Figure 27: This is the data for the representative device temperature vs time with the Nomex laminate on top of the representative device to shield it from the heat flux at 20 kW/m². Highlighted in red is the success time for this test.

As can be seen from the results of this test, it took approximately 34 seconds for the representative device to reach 35°C and approximately 53 seconds for the representative device temperature to reach 45°C.

Following the Nomex laminate test, the next test conducted was the AS fiberglass laminate. This laminate was slightly thicker than the Nomex Laminate, with a thickness of 1.6 mm. The test was performed in the back orientation, with the screen face down and the laminate above the representative device covering the back surface from the incoming heat flux. The data collected from this test is in Figure 28 below.

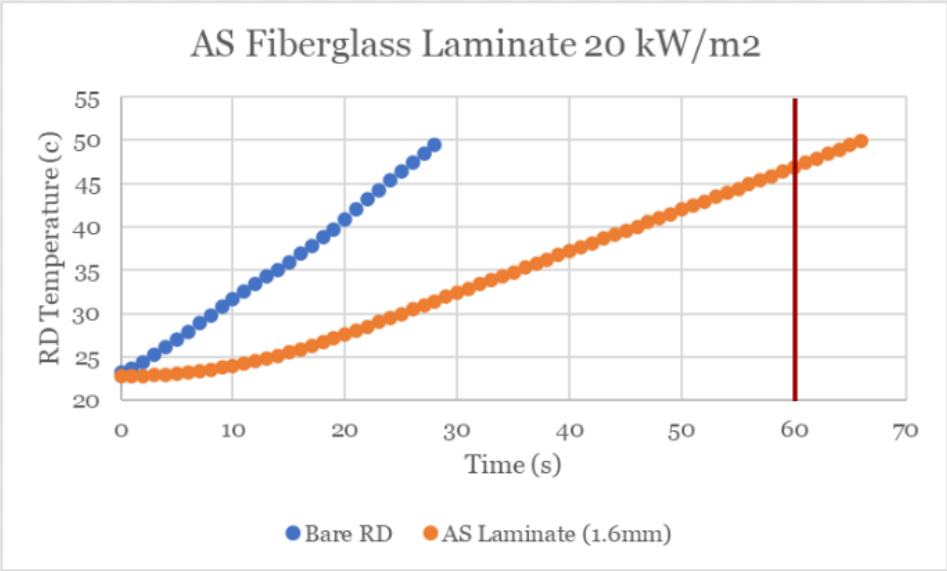

Figure 28: This is the data for the representative device temperature vs time with the AS fiberglass laminate on top of the representative device to shield it from the heat flux at 20 kW/m^2. Highlighted in red is the success time for this test.

The results of this test show that it took approximately 35 seconds for the representative device to reach 35^{o}C and approximately 56 seconds for the representative device to reach 45^{o}C.

Phase Change Material, 20 kW/m^2

Following the laminate testing, the next tests that were performed were the phase change material tests. The first one conducted was with the PCM in the front orientation. This consists of the screen side of the bare representative device directly getting the heat flux applied to it with the cone heater, with the PCM below the representative device on the back side. The goal of this test was to see if the PCM would be able to channel heat out of the representative device into the PCM below. The PCM layer used was 7 mm thick, the same thickness as the thermal pathing, however this was not included as thickness due to its not being between the heat flux and the representative device. The orientation of this test is included in Figure 29, and the results are included in Figure 30.

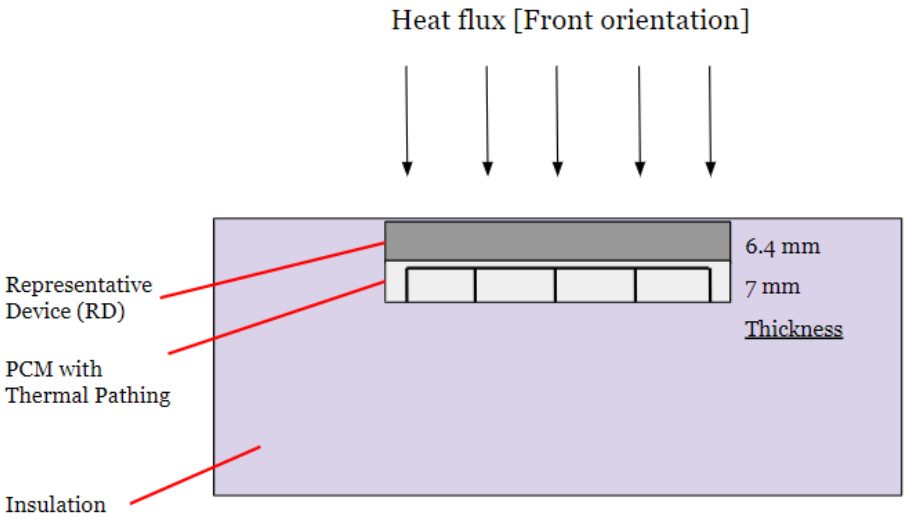

Figure 29: The testing setup for the PCM only test in the front orientation. This figure is not made to scale.

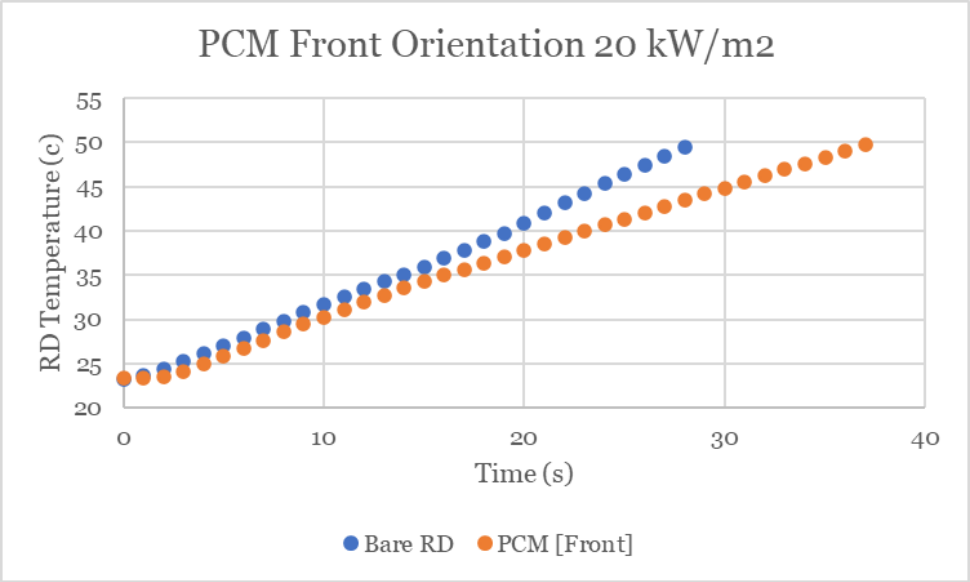

Figure 30: This is the data for the representative device temperature vs time with the PCM beneath the representative device in the Front orientation at 20 kW/m^2.

The results of this test show that there was a slightly better performance with the PCM below the representative device. It took approximately 16 seconds for the representative device to reach a temperature of 35°C and approximately 23 seconds for the representative device to reach 45°C.

The next test performed was a test with the phase change material in the back orientation with the screen side down and the PCM above the representative device. The PCM layer used was 7 mm thick, the same thickness as the thermal pathing. The orientation of this test setup is given in Figure 31, while the results of the test are given in Figure 32.

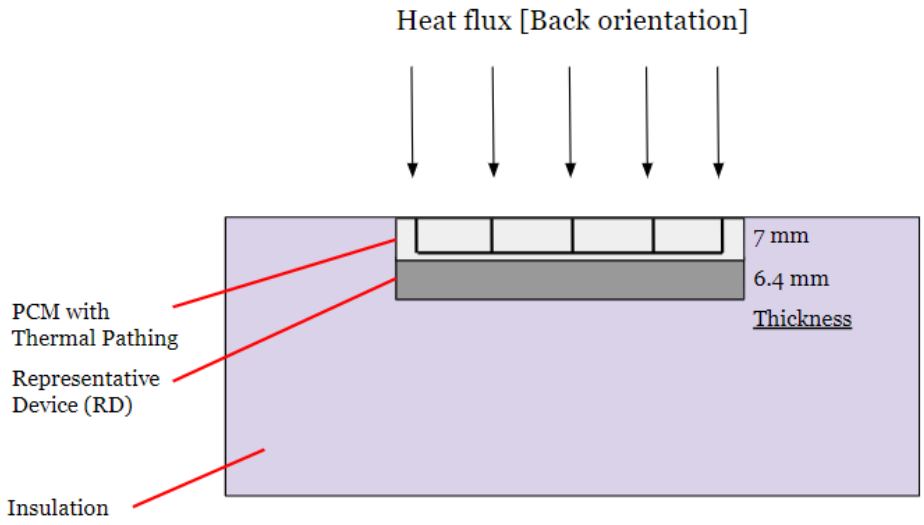

Figure 31: The testing setup for the PCM only test in the back orientation. This figure is not made to scale.

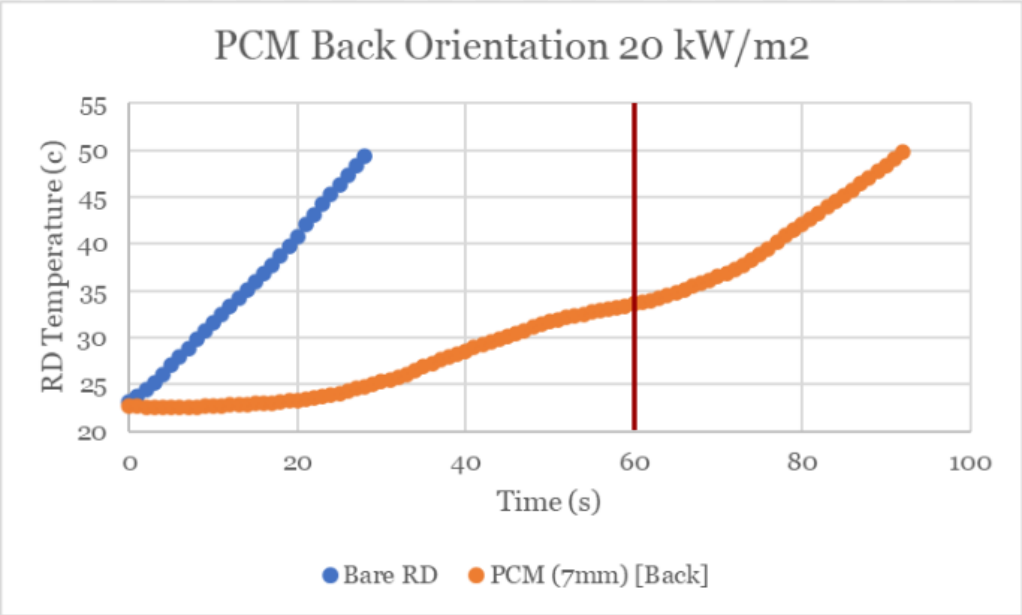

Figure 32: This is the data for the representative device temperature vs time with the PCM above the representative device in the back orientation at 20 kW/m^2. Highlighted in red is the success time for this test.

The representative device took 66 seconds to reach the temperature of 35^{o}C, and it took 85 seconds for the representative device to reach 45^{o}C. The PCM layer above the representative device was very effective at stopping heat from entering the representative device.

Combined Testing, 20 kW/m²

The final two tests performed at 20 kW/m² were the two combined tests. The first of these tests was a PCM Borofloat test. This test was conducted in the front orientation. Here, the Borofloat was on the screen side above the representative device, and the phase change material was below to channel heat out of the representative device. The orientation of this test can be seen in Figure 33, and the results of this test can be seen in Figure 34.

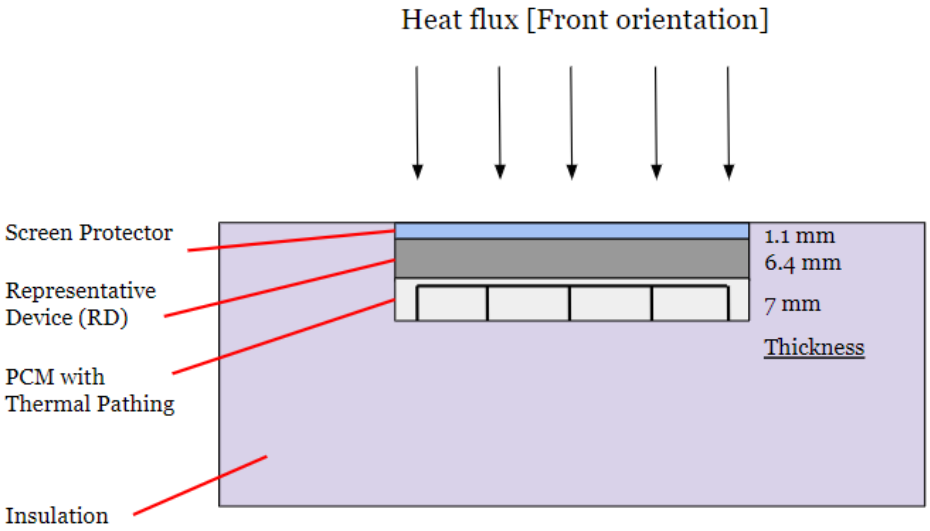

Figure 33: The testing setup for the PCM and Borofloat test in the front orientation. This figure is not made to scale.

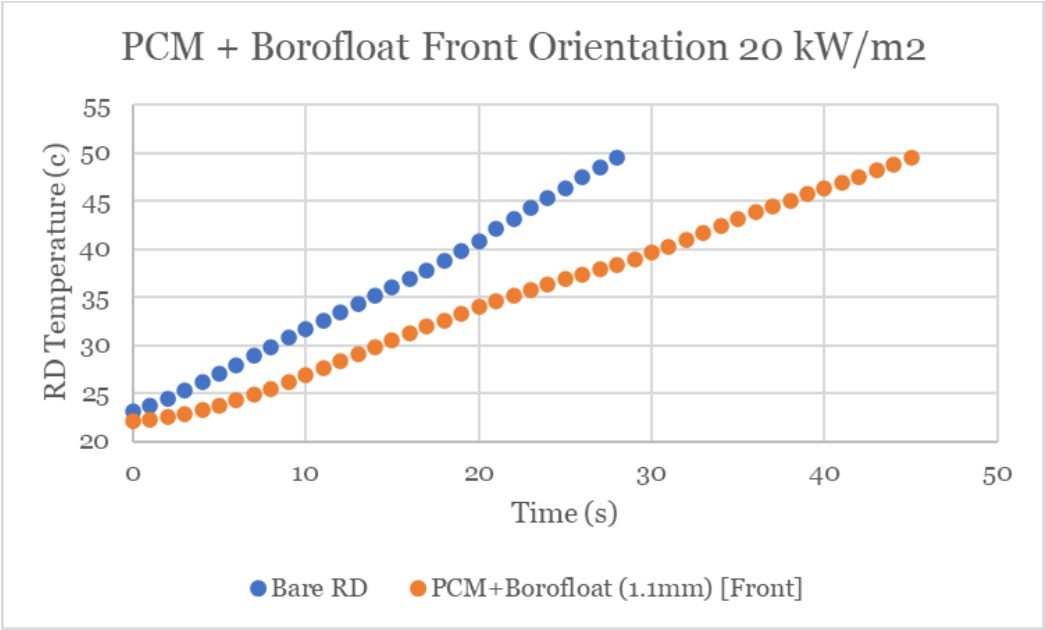

Figure 34: This is the data for the representative device temperature vs time with the PCM beneath the representative device and the glass above the representative device in the front orientation at 20 kW/m². Only the glass thickness is considered as the PCM is beneath the representative device.

It can be seen in the figure that it took approximately 22 seconds for the representative device temperature to reach 35°C and approximately 31 seconds for the representative device to reach 45°C. This performed much lower than originally anticipated in the simulation which predicted 153 seconds. This could be due to several factors, including a lack of sufficient thermal contact between the PCM and the RD, due to our thermal pathing, or a loss of PCM through drippage in our setup.

Following this test, the final 20kW/m² test was conducted. This test was conducted in the back orientation with the screen side down. The PCM was above the representative device, and the AS fiberglass laminate was above the PCM. The laminate shielded both the PCM and the representative device from the heat flux, slowing the rate at which the PCM melts. The PCM and laminate together had a thickness of 8.6 mm. The orientation of this test is given in Figure 35, while the results of the test are in Figure 36.

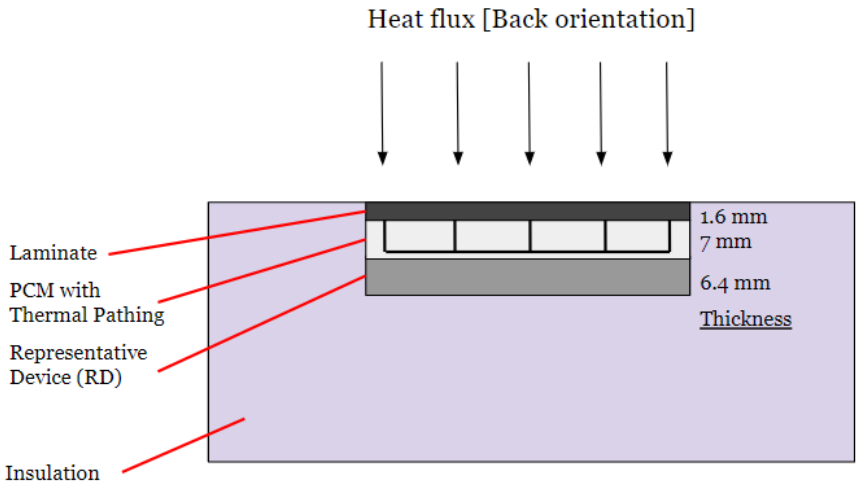

Figure 35: The testing setup for the PCM and AS fiberglass laminate test in the back orientation. This figure is not made to scale.

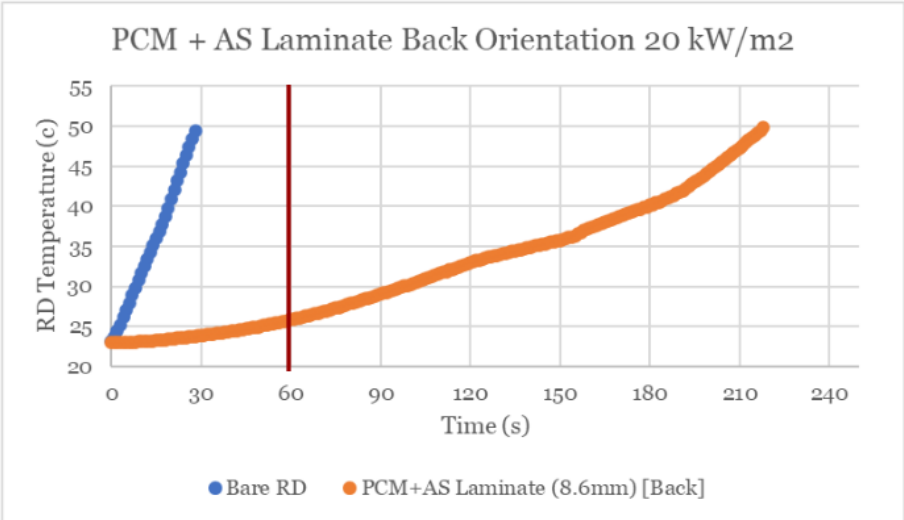

Figure 36: This is the data for the representative device temperature vs time with the PCM above the representative device in the front orientation at 20 kW/m^2. Above the PCM is the AS fiberglass laminate. The thickness is 8.6 mm because the PCM is 7 mm thick while the AS laminate is 1.6mm thick. Highlighted in red is the success time for this test.

The results of this test show that it took 142 seconds for the representative device to reach 35^{o}C, and it took 203 seconds for the representative device to reach 45^{o}C. The laminate did take some damage from this test. The same laminate was used for this test as for the other 20 kW/m^2 laminate test, as well as for the 70 kW/m^2 laminate test. Going into this test, the laminate had already been exposed to some minor cracking and discoloration from the 70 kW/m^2 test. Following this test, there was greater cracking and discoloration in the laminate. The before and after photos of the laminate from this test are included below.

Figure 37: Before (left) and after (right) photos of the AS fiberglass laminate following the test with the PCM and the laminate conducted at 20 kW/m^2.

Bare RD, 70 kW/m^2

The first test to be performed at 70 kW/m^2 was the bare representative device test. This test serves as the benchmark for all the following tests performed at 70 kW/m^2. The orientation of this test is included below, and the results of this test can be seen in Figure 39.

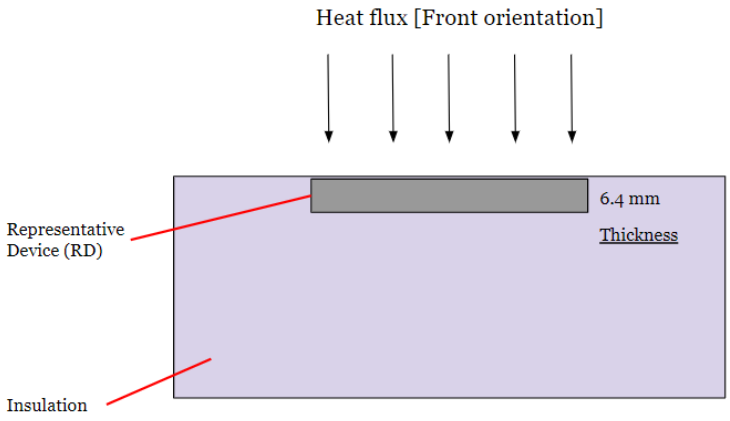

Figure 38: The testing setup used for the bare representative device test. This figure is not made to scale.

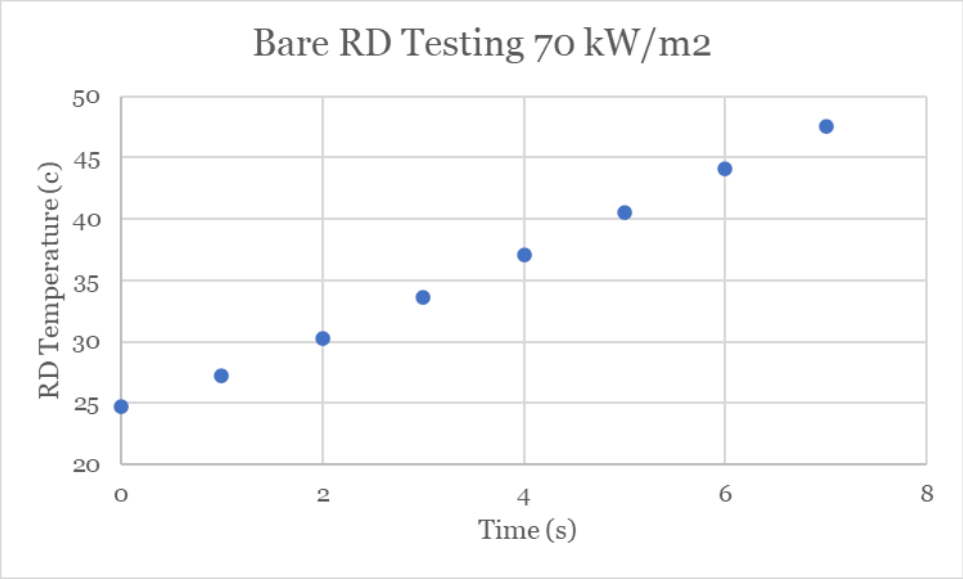

Figure 39: This is the data for the representative device temperature vs time without any measures being used to protect it from the heat flux at 70 kW/m^2.

For the bare representative device test, it took approximately 3.5 seconds to reach 35^{o}C and just over 6 seconds to reach 45^{o}C.

Glass Screen Protectors, 70 kW/m^2

The first glass material tested at the 70 kW/m^2 heat flux was the Borofloat. This material was tested in the front orientation, and had a thickness of 1.1 mm. The orientation used for this test is in Figure 40, while the results of this test are in Figure 41.

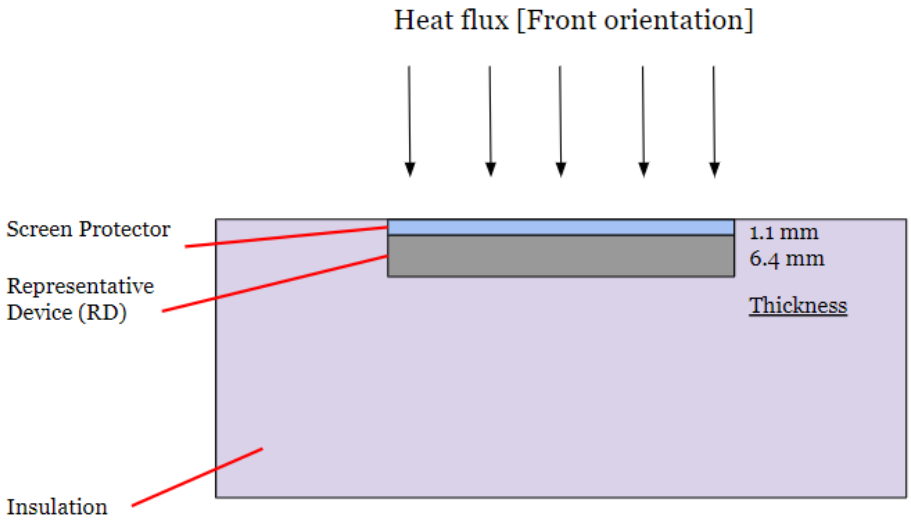

Figure 40: The orientation of the setup used for both the Borofloat and the soda lime glass tests. This figure is not made to scale.

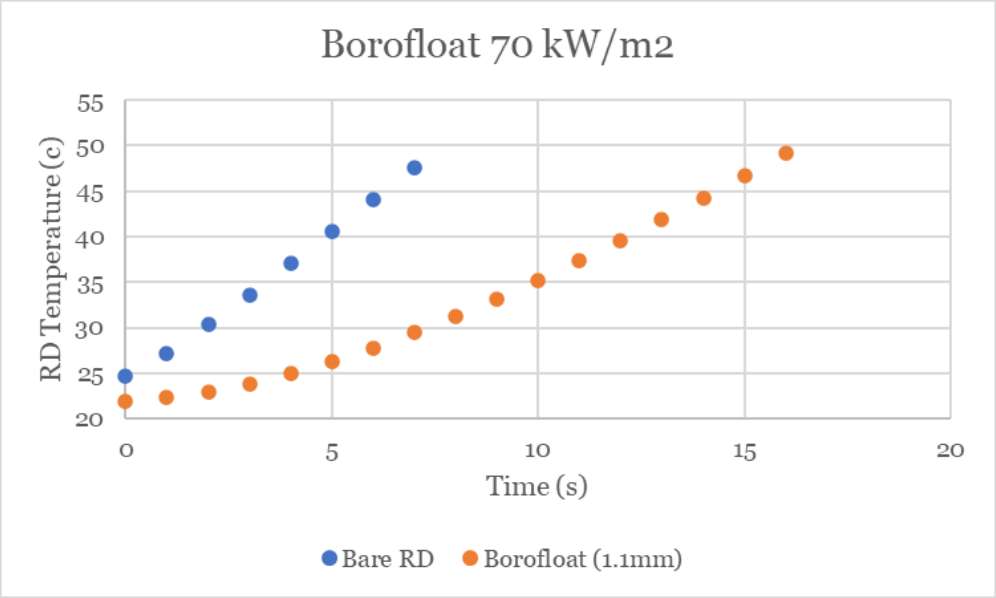

Figure 41: This is the data for the representative device temperature vs time with the Borofloat glass on top of the representative device to shield it from the heat flux at 70 kW/m^2.

It took 10 seconds for the representative device to reach the temperature of 35^{o}C and approximately 14 seconds for the representative device to reach the 45^{o}C.

The following test was for the soda lime glass. Like the Borofloat glass, it has a thickness of 1.1 mm and the test was conducted in the front orientation. The results of this test are included in Figure 42.

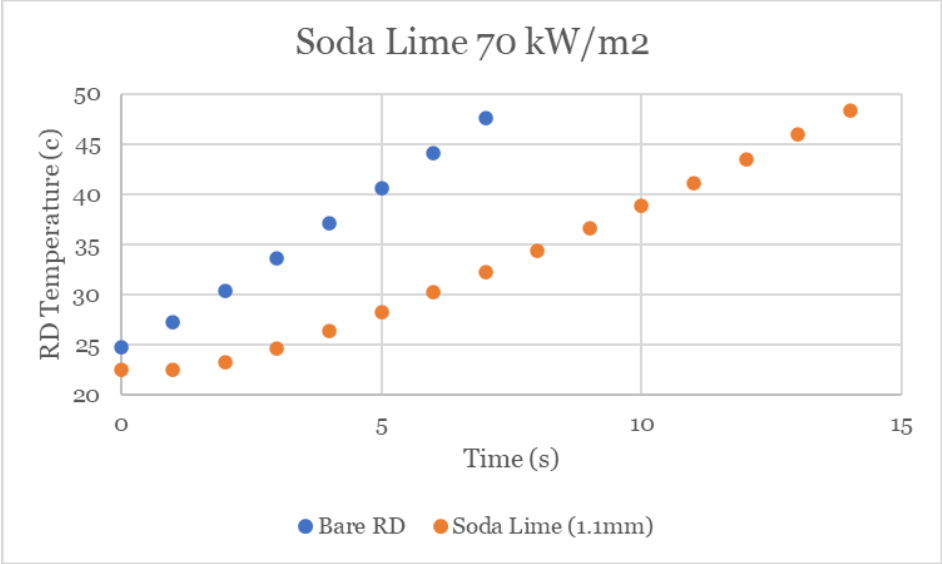

Figure 42: This is the data for the representative device temperature vs time with the soda lime glass on top of the representative device to shield it from the heat flux at 70 kW/m^2.

The results of this test show that it took approximately 8 seconds for the representative device to reach 35^{o}C and approximately 12.5 seconds for the representative device to reach 45^{o}C.

Fabrics, 70 kW/m²

The next category of materials tested was fabrics. All three fabrics were tested at 70 kW/m². The first one tested was the Nomex fabric. This test was conducted with the back orientation and the Nomex fabric had a thickness of 0.5 mm. The orientation of the testing apparatus is given in Figure 43, while the results of this test can be seen in Figure 44.

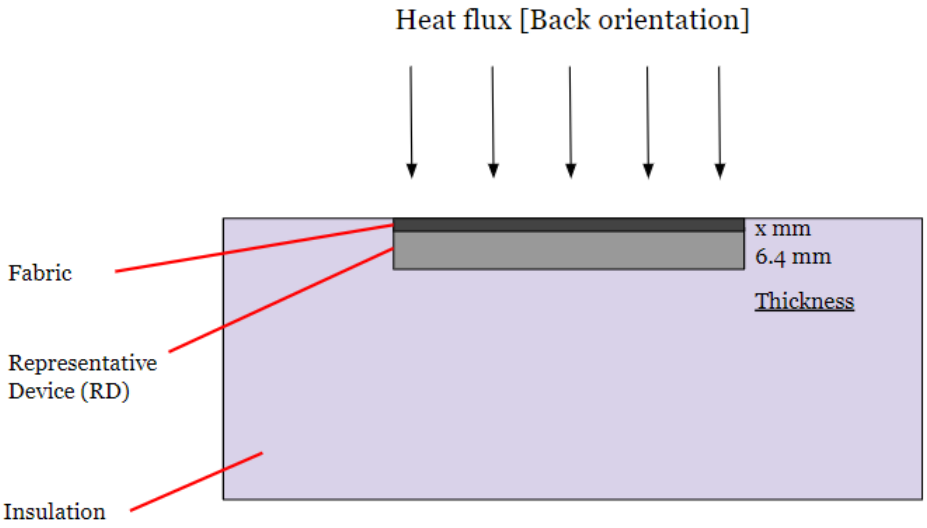

Figure 43: The test setup orientation for the fabric tests. For the Nomex, x is 0.5 mm. For the AS fiberglass, x is 0.85. For the GL fiberglass, x is 0.4 mm. This figure is not made to scale.

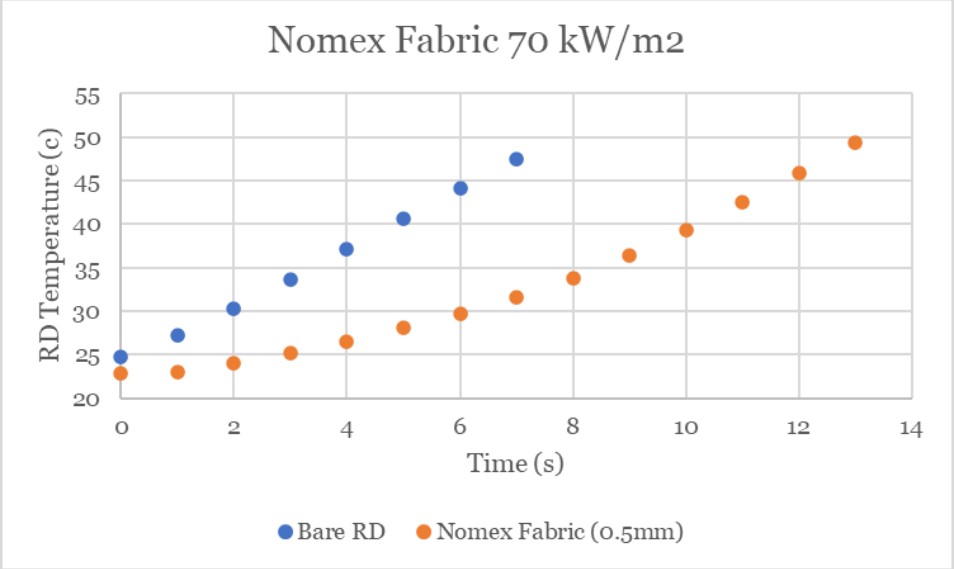

Figure 44: This is the data for the representative device temperature vs time with the Nomex Fabric on top of the representative device to shield it from the heat flux at 70 kW/m².

From this test, it took the representative device approximately 8.5 seconds to reach 35°C and approximately 12 seconds to reach 45°C. It is important to note that at approximately the 8 second mark during this test, the Nomex fabric failed and combusted. The Nomex fabric began to curl

following ignition, and was allowed to burn out under the heater. The Nomex before the test and the Nomex burning are pictured below.

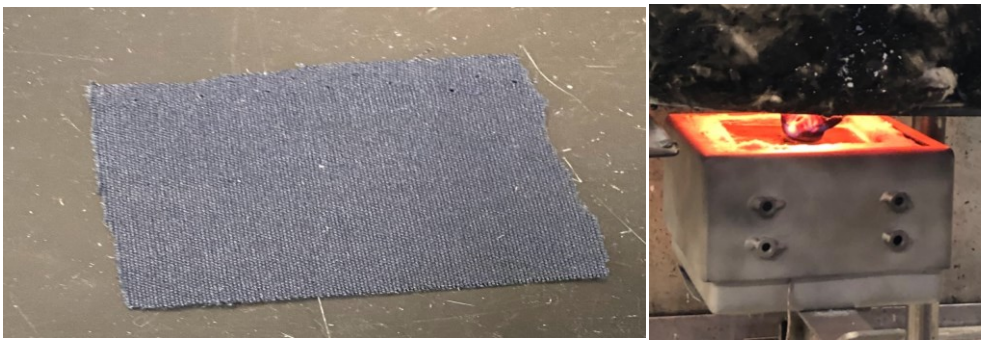

Figure 45: The Nomex fabric before the 70 kW/m² test and while it was allowed to burn out under the cone heater.

Following the Nomex fabric test, the next test conducted was the GL fiberglass fabric at 70 kW/m². This fabric had a thickness of 0.4 mm and the test was conducted in the back orientation. The results of this test can be seen below.

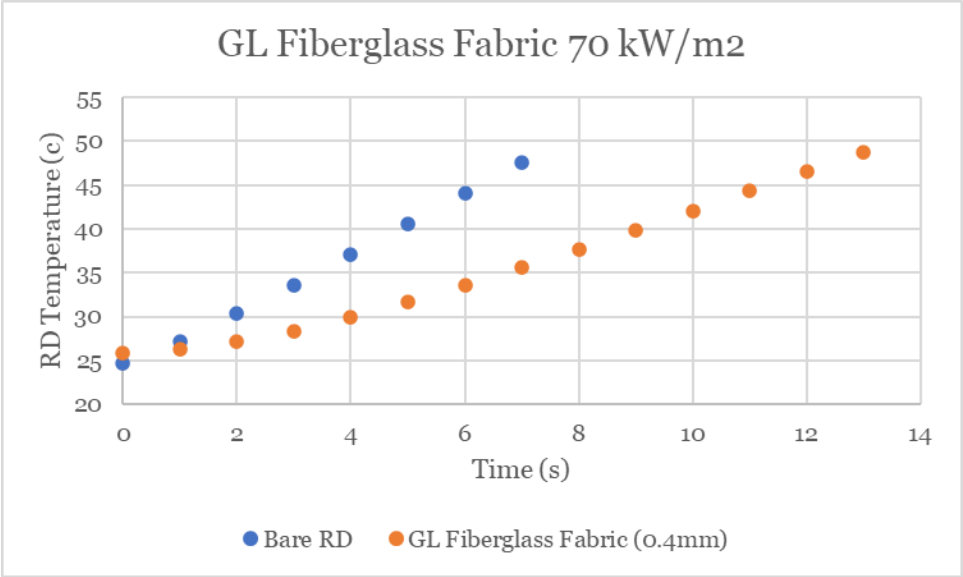

Figure 46: This is the data for the representative device temperature vs time with the GL fiberglass fabric on top of the representative device to shield it from the heat flux at 70 kW/m².

It can be seen from Figure 46 that with the GL fiberglass fabric it took approximately 7 seconds for the representative device to reach 35°C and approximately 11 seconds for it to reach 45°C.

The final fabric tested at 70 kW/m² was the AS fiberglass fabric. This test was done in the back orientation, and this fabric has a thickness of 0.85 mm. The results of this test are in Figure 47 below.

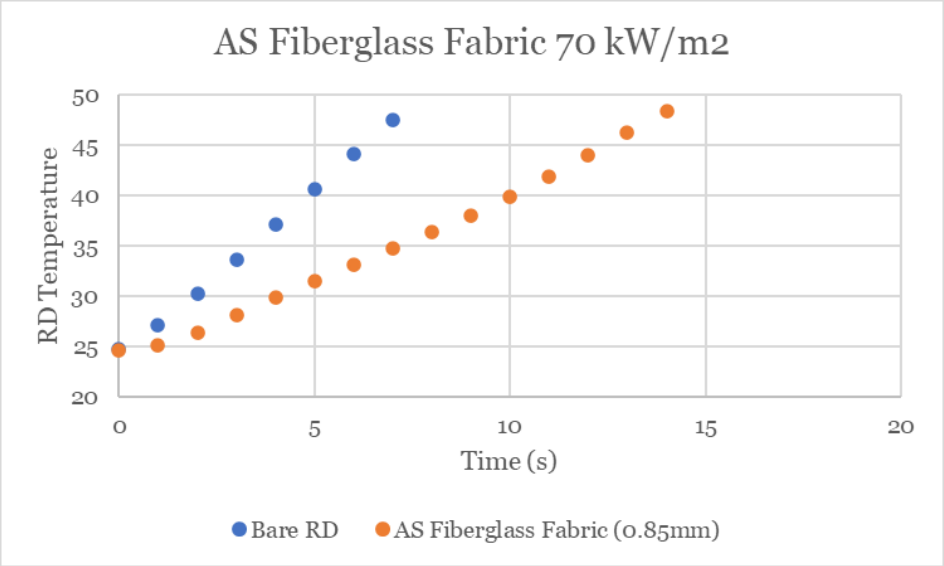

Figure 47: This is the data for the representative device temperature vs time with the AS fiberglass fabric on top of the representative device to shield it from the heat flux at 70 kW/m^2.

It took approximately 7 seconds for the representative device to reach 35^{o}C, and approximately 12 seconds for the representative device to reach 45^{o}C.

Laminates, 70 kW/m^2

Two laminates were tested at 70 kW/m^2. The first was the Nomex laminate. This was tested in the back orientation, and this laminate had a thickness of 1.5 mm. The testing orientation is given in Figure 48, while the results of the test are given in Figure 49.

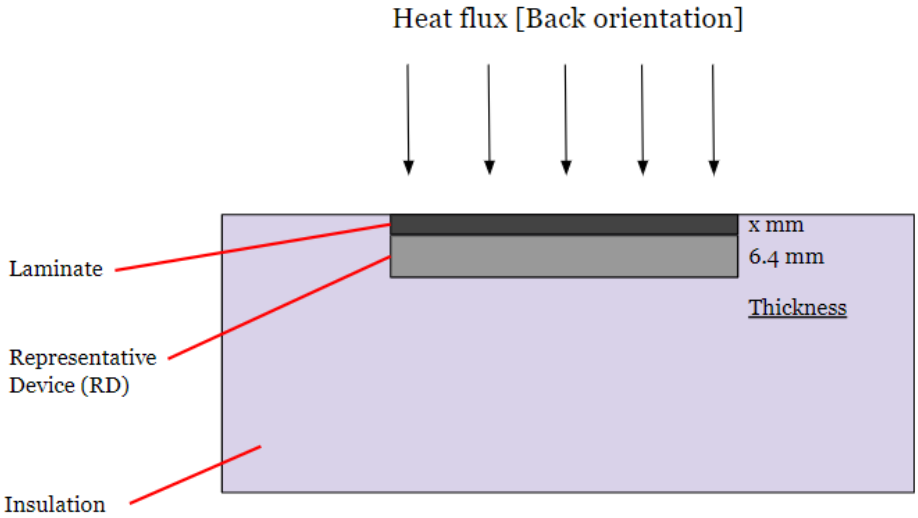

Figure 48: The orientation for the laminate tests. For the Nomex laminate, x is 1.5 mm, while for the AS fiberglass laminate test, x is 1.6mm. This figure is not made to scale.

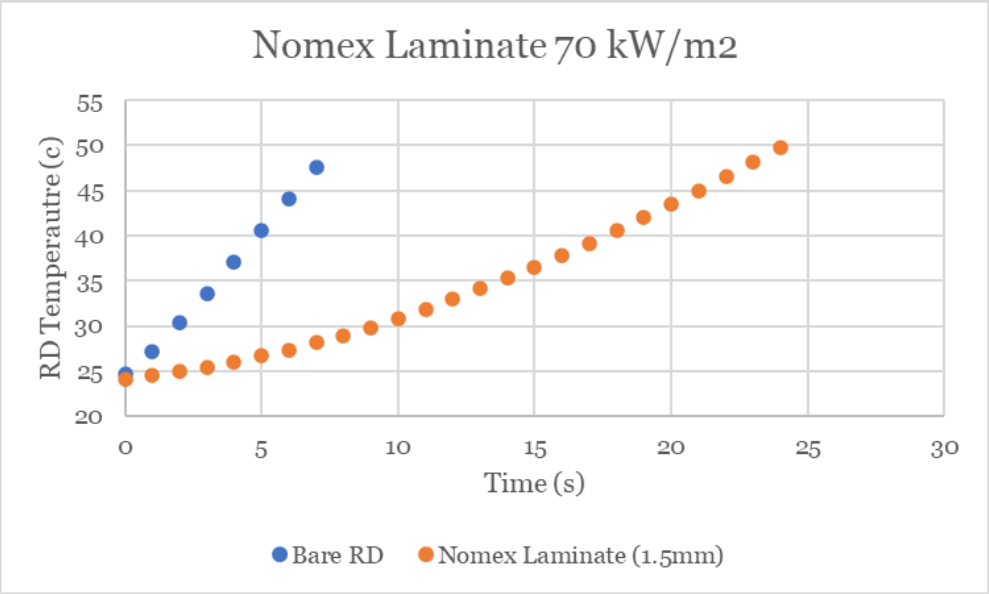

Figure 49: This is the data for the representative device temperature vs time with the Nomex laminate on top of the representative device to shield it from the heat flux at 70 kW/m^2.

This figure shows that it took approximately 14 seconds for the representative device to reach 35^{o}C, and approximately 21 seconds for it to reach 45^{o}C. The Nomex laminate did take some damage from this test, but not to the same degree as the Nomex fabric that burned away. The before and after photos of the Nomex laminate from this test can be seen below, showing the discoloration of the Nomex laminate following this test.

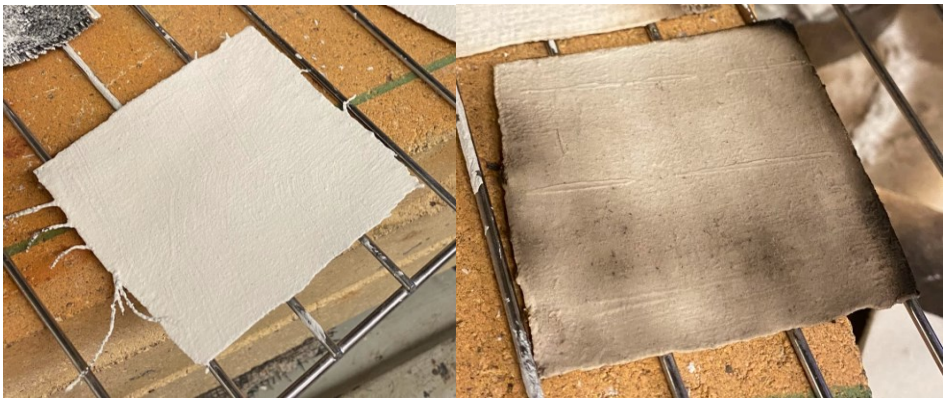

Figure 50: Before (left) and after (right) photos of the Nomex laminate following the test conducted at 70 kW/m^2.

The next test performed was a test with the AS fiberglass laminate. This laminate has a thickness of 1.6 mm and the test was conducted in the back orientation with the screen side down and the laminate on top of the representative device. The results of this test are shown below.

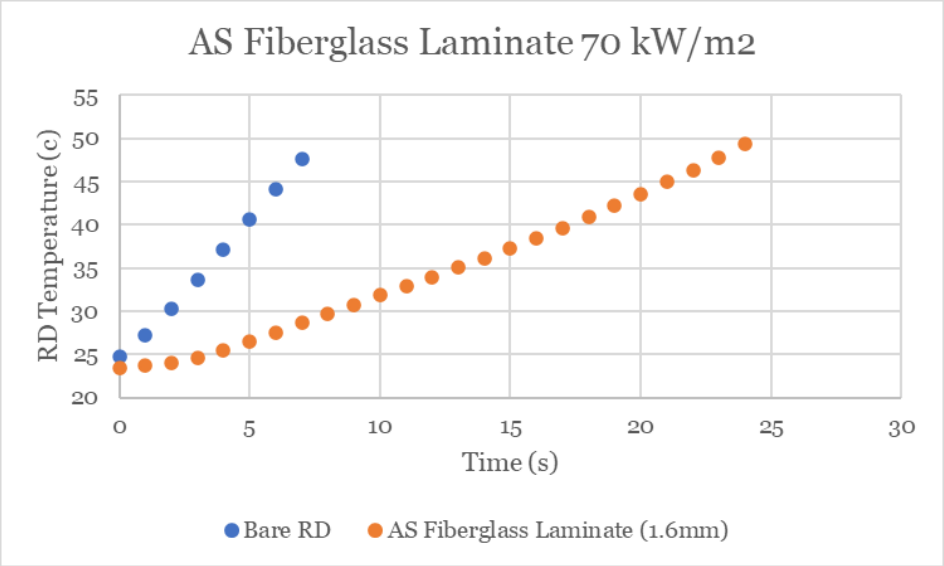

Figure 51: This is the data for the representative device temperature vs time with the AS fiberglass laminate on top of the representative device to shield it from the heat flux at 70 kW/m^2.

It can be seen from the figure above that the representative device reached 35^{o}C after 13 seconds, and it took 21 seconds to reach 45^{o}C. This laminate also took minor damage, but not as much as the Nomex laminate. The laminate showed minor cracking of the exterior layer and had a minor scorch in one corner. Notably, this location is where a test was conducted to see if the melted phase change material would be absorbed into the laminate. The result of this test showed that about 30% of the PCM applied to the laminate was absorbed into it. It is reasonable to conclude that PCM within the laminate contributed to the greater damage at that location of the laminate.

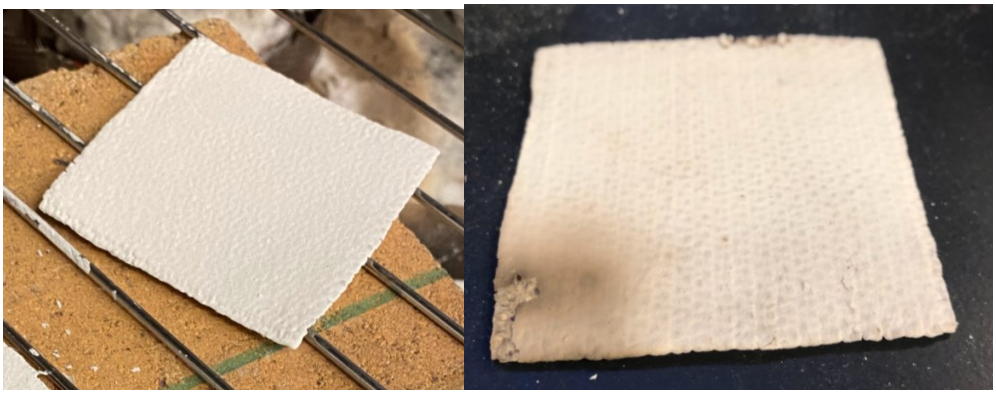

Figure 52: Before (left) and after (right) photos of the AS fiberglass laminate following the test with just the laminate conducted at 70 kW/m^2.

Phase Change Material, 70 kW/m^2

Only one test was performed with just the phase change material. This was the test for the PCM in the front orientation. This test had the representative device taking the 70 kW/m^2 heat flux directly, with the PCM beneath trying to channel the heat out of the representative device. The orientation of the testing apparatus is given in Figure 53, while the results of this test can be seen in Figure 54.

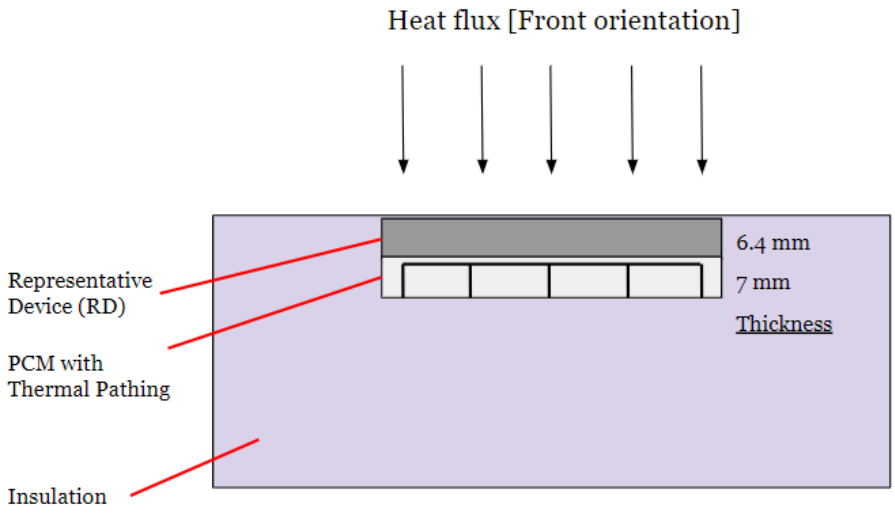

Figure 53: The testing setup for the PCM only test in the front orientation. This figure is not made to scale.

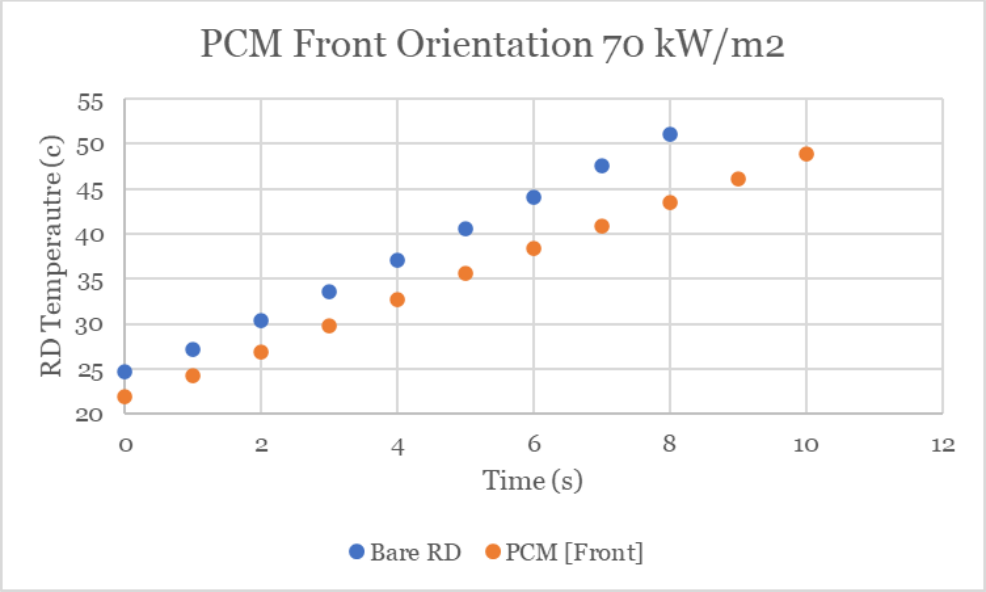

Figure 54: This is the data for the representative device temperature vs time with the PCM beneath the representative device in the Front orientation at 70 kW/m^2.

The results of this test show that it took 5 seconds for the representative device to reach 35^{o}C and approximately 8.5 seconds for the PCM to reach 45^{o}C. It is important to note that the representative device started at 22^{o}C for the PCM test where it was approximately 24.5^{o}C in the bare representative device test. Based on the slopes of these graphs, the PCM made no noticeable difference in the data collected. Additionally, this test resulted in ignition of the PCM. At the 12 second mark, as the testing apparatus was about to be removed from the cone heater, combustion began. As per protocol, we initially intended to let it burn out to prevent spillage of a flaming

liquid. However, over time the fire became larger and the decision was made to remove the apparatus from the heater. Pictures of the fire can be seen in the figure below.

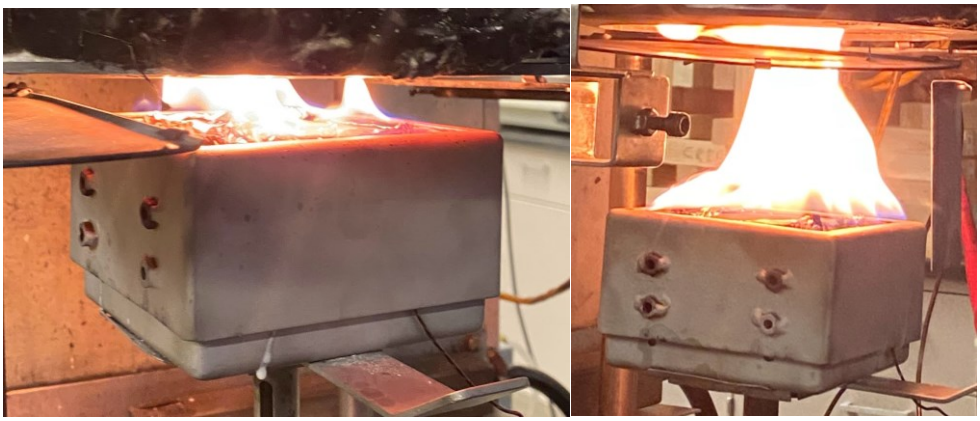

Figure 55: The PCM fire that occurred while doing the front orientation PCM test at 70 kW/m^2.

Following this fire, we elected to not do an equivalent test in the back orientation. Fire had been an anticipated risk before testing, and we predicted that the laminate shielding the PCM would prevent the PCM from igniting. Because of this, the PCM and laminate test was the only other test that we performed with the PCM at 70 kW/m^2.

Combined Testing, 70 kW/m^2

The final test was the PCM laminate test. Here we had the AS fiberglass laminate and the PCM both above the representative device in the back orientation. The total thickness of the PCM and the AS laminate is 8.6 mm. The orientation used for this test is given in Figure 56, while the data for this test can be seen in Figure 57.

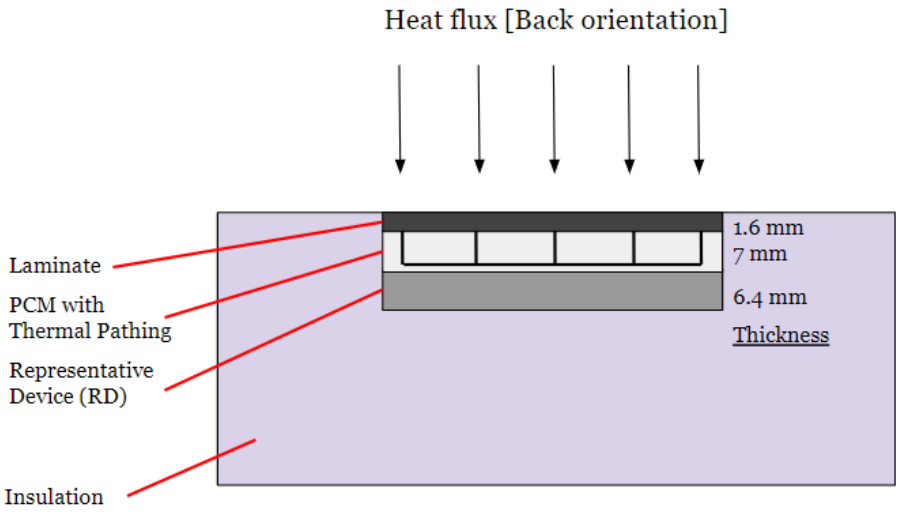

Figure 56: The testing setup for the PCM and AS fiberglass laminate test in the back orientation. This figure is not made to scale.

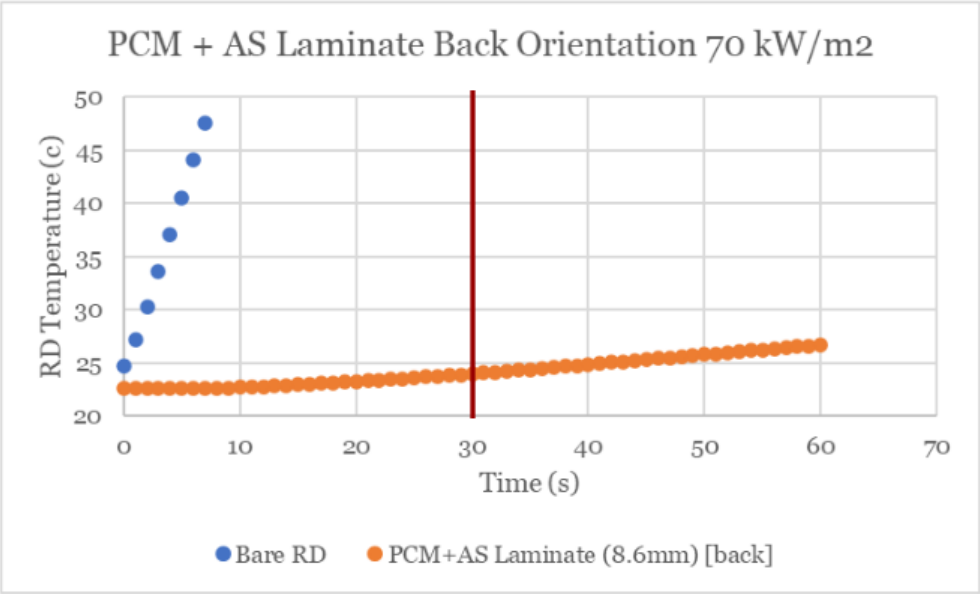

Figure 57: This is the data for the representative device temperature vs time with the PCM above the representative device in the back orientation at 20 kW/m^2. Above the PCM is the AS fiberglass laminate. The thickness is 8.6 mm because the PCM is 7 mm thick while the AS laminate is 1.6mm thick. Highlighted in red is the success time for this test.

It can be seen in the figure above that the representative device never reached 35^{o}C, as we pulled the apparatus out of the cone heater after 1 minute had passed. This was done because the metric for success had already been far surpassed, and we did not want to risk a PCM fire. This test did lead to the failure of the AS fiberglass laminate. While it did not combust, it was scorched to the point where it was deemed that it would no longer be viable for further testing. It is important to note that the laminate was pushed far past conditions that are normal. One minute of 70 kW/m^2 is far beyond what is survivable by a human, thus it should not be expected for the laminate to be exposed to this heat flux for this length of time. The before and after photos of the laminate are included below.

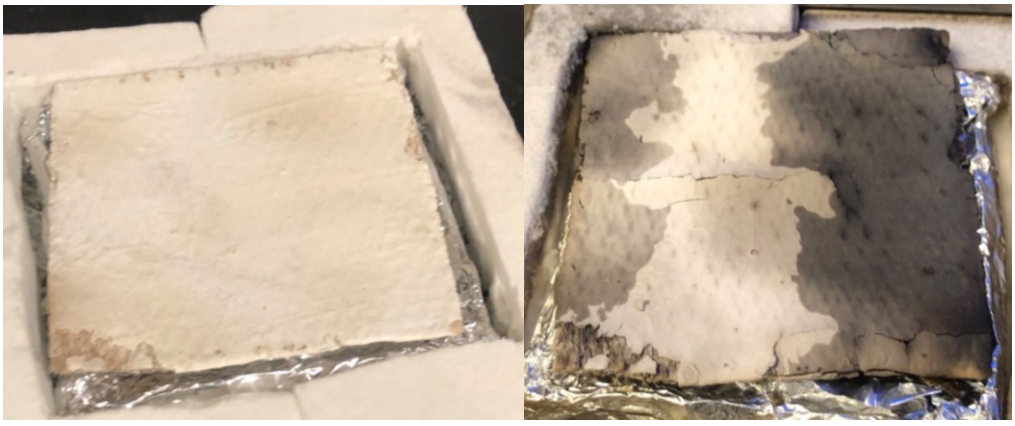

Figure 58: Before (left) and after (right) photos of the AS fiberglass laminate following the test conducted with the PCM and the laminate at 70 kW/m^2.

Discussion

Glass 20 kW/m²

The first category of tests performed at 20 kW/m² was the glass tests. It can be seen from Figure 59 that the Borofloat and the soda lime glass had near identical performances. While they both performed practically the same, the Borofloat still has better thermal properties, and is more resistant to thermal stresses. Neither of these materials met the 60 seconds to hit 45°C that was deemed a success for the 20 kW/m² tests.

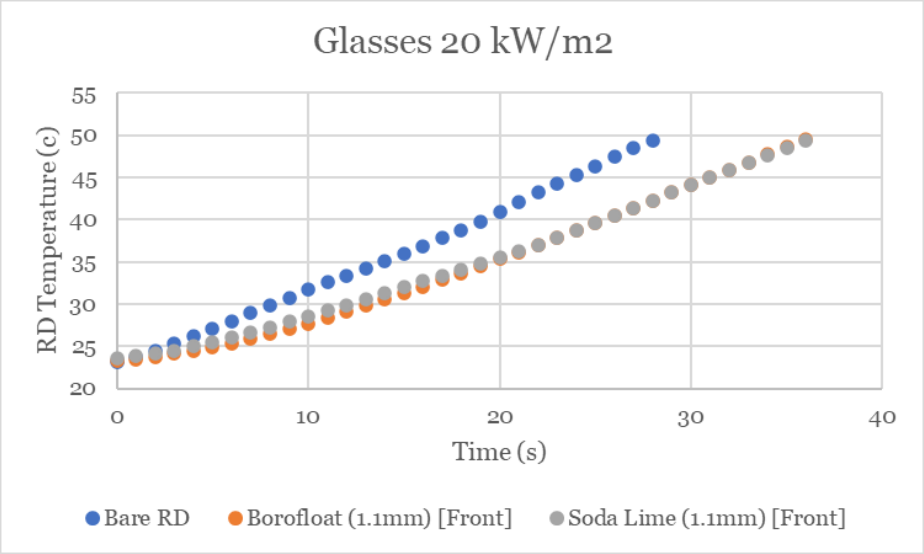

Figure 59: The combined data for the bare RD and both glass tests performed at 20 kW/m².

Fabric 20 kW/m²

The next category of 20 kW/m² tests was the fabrics. The compounded results of these tests can be seen in Figure 60. For these tests, the AS fiberglass performed the best. This makes sense, as it is the thickest of these materials. The next best performance was from the Nomex fabric; however, this material was damaged by the heat flux while the fiberglass fabrics were not. The GL fiberglass fabric was the worst performing of the fabrics; however, it was also thinner. None of the fabric materials met the 60 seconds under the 20 kW/m² to be deemed a success.

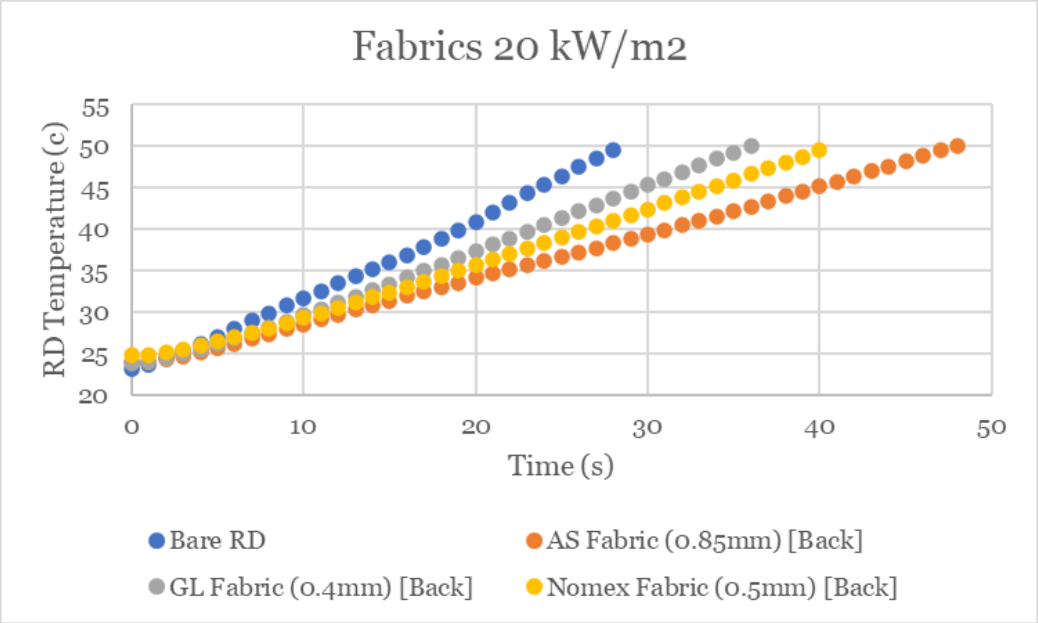

Figure 60: The combined data for the bare RD and the fabric tests at 20 kW/m².

Laminate 20 kW/m²

The third material category tested was the laminates. The two laminates that were tested were the Nomex laminate and the AS fiberglass laminate. Both materials had comparable performances at this heat flux, and neither was damaged. Neither laminate met the metric of 60 seconds to hit 45°C that was deemed a success for the 20 kW/m² testing. The laminate results are included in Figure 61.

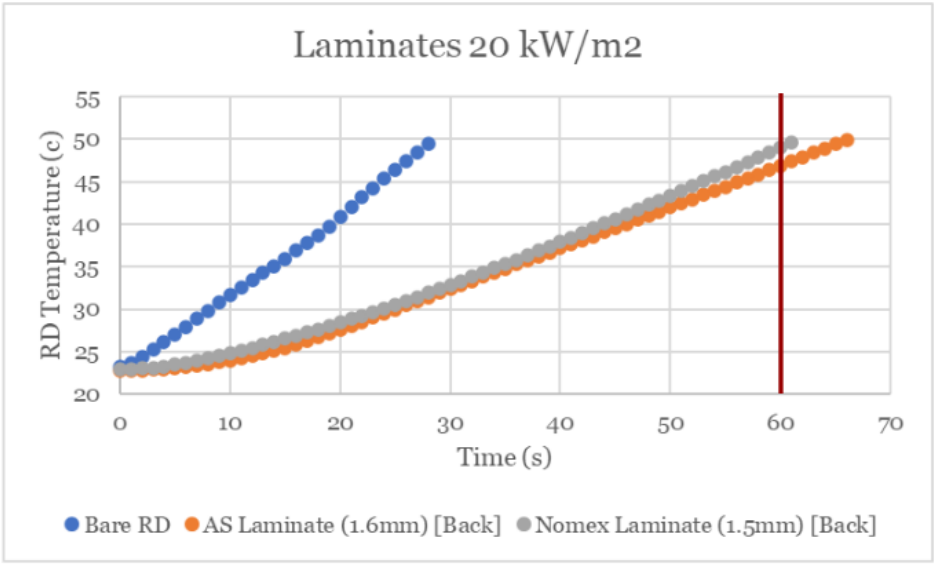

Figure 61: The combined data for the bare RD and the laminate tests at 20 kW/m². Highlighted in red is the success time for these tests.

PCM Front Orientation 20 kW/m²

While tests were categorized as PCM tests and combined tests during the testing phase, it makes more sense in analysis to compare the PCM and combined tests that were performed in the front orientation and the PCM and combined tests that were conducted in the back orientation. The first category examined here is the PCM front orientation tests. Additionally, the Borofloat only test was also included on the graph to show how the addition of PCM made a difference in the Borofloat and PCM combined test. It can be seen from the comparison of these tests that the PCM provided marginal improvements compared to the bare representative device and the Borofloat tests. However, this marginal difference was not enough that either of these tests was able to meet the 60 seconds to reach the 45°C parameter. These results are in Figure 62 below.

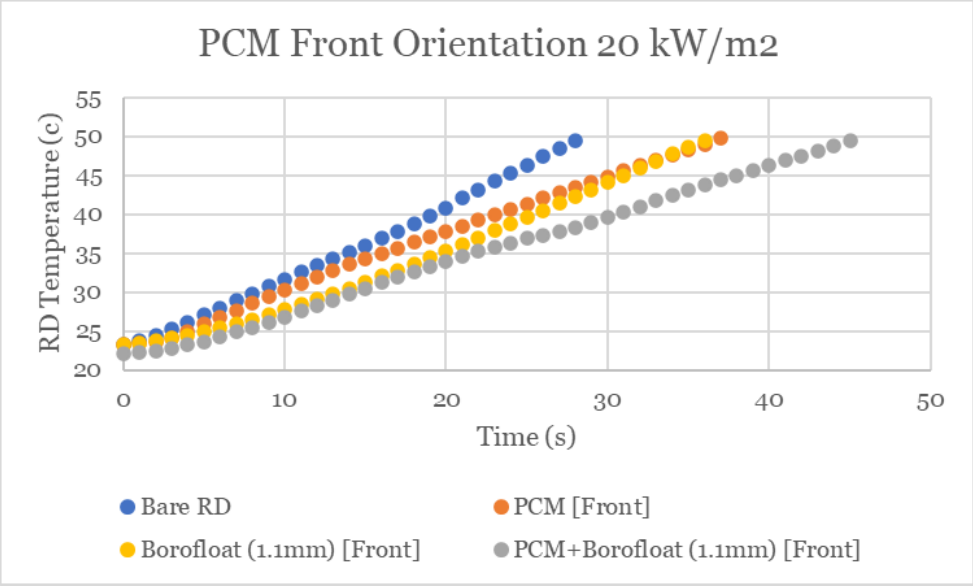

Figure 62: The combined data for the bare RD, the Borofloat test, and the front orientation PCM tests at 20 kW/m².

PCM Back Orientation 20 kW/m²

This category has the results of the back orientation tests, as well as the bare RD test and the AS fiberglass laminate test for comparison. It can be seen here that the PCM alone outperformed the AS fiberglass laminate alone. Additionally, it can be seen in the figure below that the combined test with both the PCM and the laminate performed better than the sum of its parts (which is to say that the time it took to reach 35°C and 45°C for the combined test was greater than the times for the laminate and the PCM individually added together). Both back orientation tests with the PCM were able to achieve the goal of 60 reach seconds to reach 45°C. To reiterate, the PCM by itself took 66 seconds to reach 35°C and 85 seconds to reach 45°C. The PCM and laminate combined test took 142 seconds to reach 35°C, and it took 203 seconds to reach 45°C. The back orientation PCM tests were the only tests conducted that were able to clear the established metric of 60 seconds to reach 45°C, though the AS fiberglass laminate by itself came close.

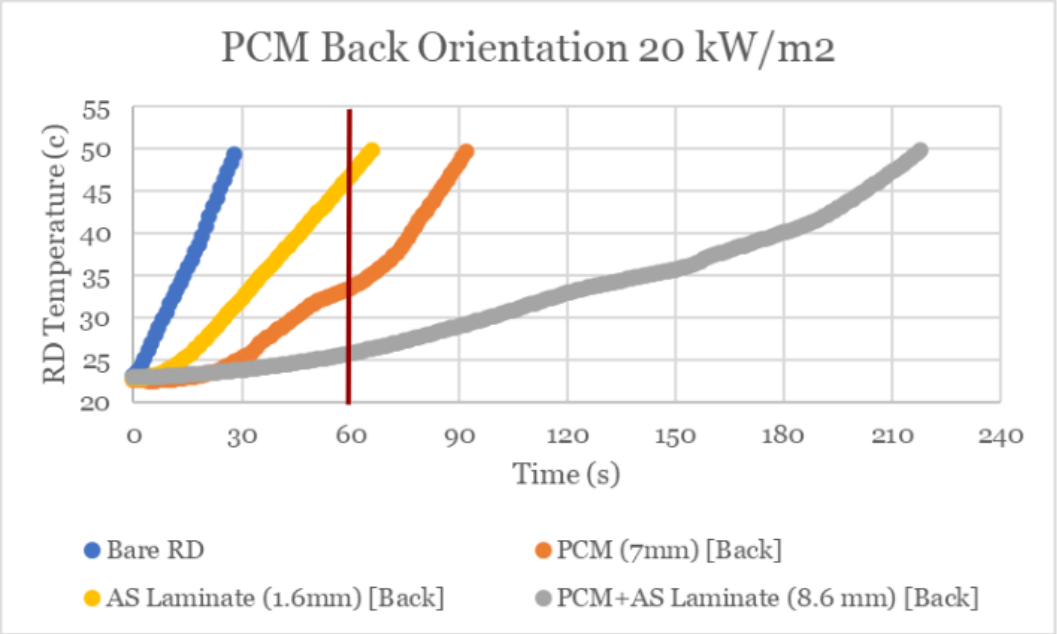

Figure 63: The combined data for the bare RD, the AS laminate, and the back orientation PCM tests at 20 kW/m². Highlighted in red is the success time for these tests.

All results 20 kW/m²

The final graph, included below, provided for the 20 kW/m² tests is a graph with the data for all the tests. It is important to note that this data is not all directly comparable. When drawing comparisons based on this chart, it is important to consider differences in material thickness between the materials between the representative device and the heat flux in each test.

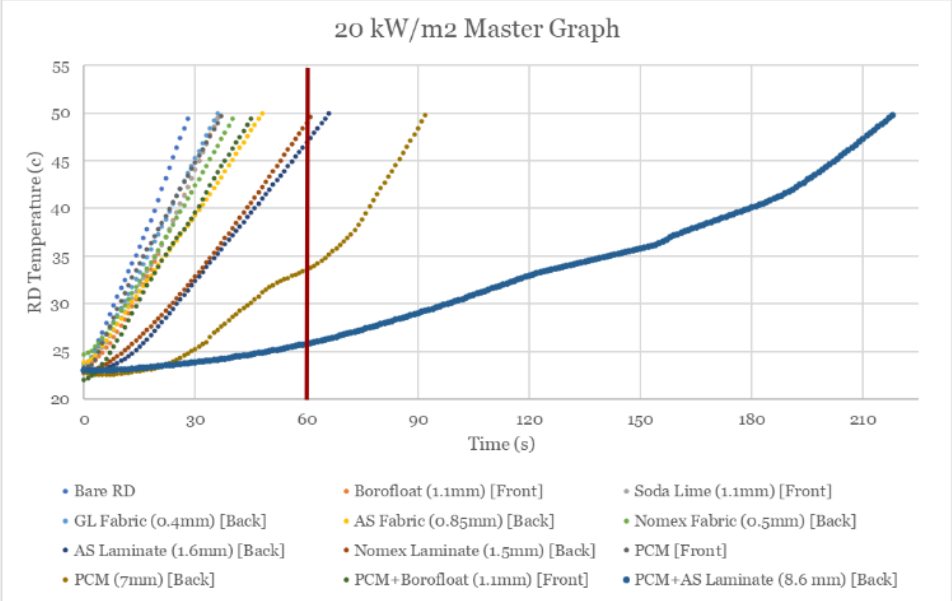

Figure 64: The combined data for all the tests conducted at 20 kW/m². Highlighted in red is the success time for these tests.

Glass 70 kW/m²

Like with the 20 kW/m² tests, the first category for 70 kW/m² was the glasses. It can be seen in the figure below that the Borofloat and the soda lime glass both performed relatively comparably at 70 kW/m², though the Borofloat did marginally outperform the soda lime glass. However, neither of these materials cleared the metric of 30 seconds under 70 kW/m².

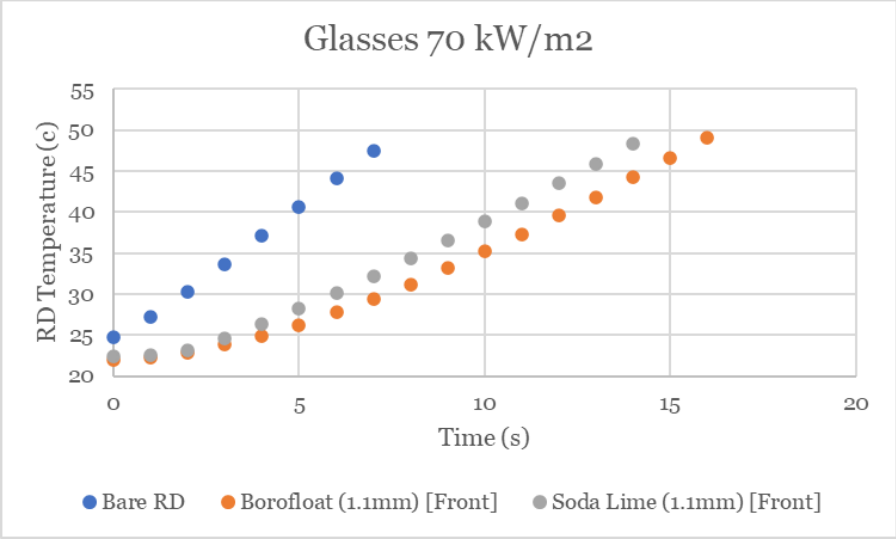

Figure 65: The combined data for the bare RD and both glass tests performed at 70 kW/m².

Fabric 70 kW/m²

For the fabrics, all three materials performed comparably at shielding the representative device from the heat flux. These materials were not considered for the design, but it is still important to assess these materials. However, it is important to note a few aspects of comparison. First, the Nomex fabric failed. Additionally, while it had a lesser performance, the GL fiberglass fabric is thinner than the AS fiberglass fabric. None of the fabric materials cleared the metric of 30 seconds under 70 kW/m².

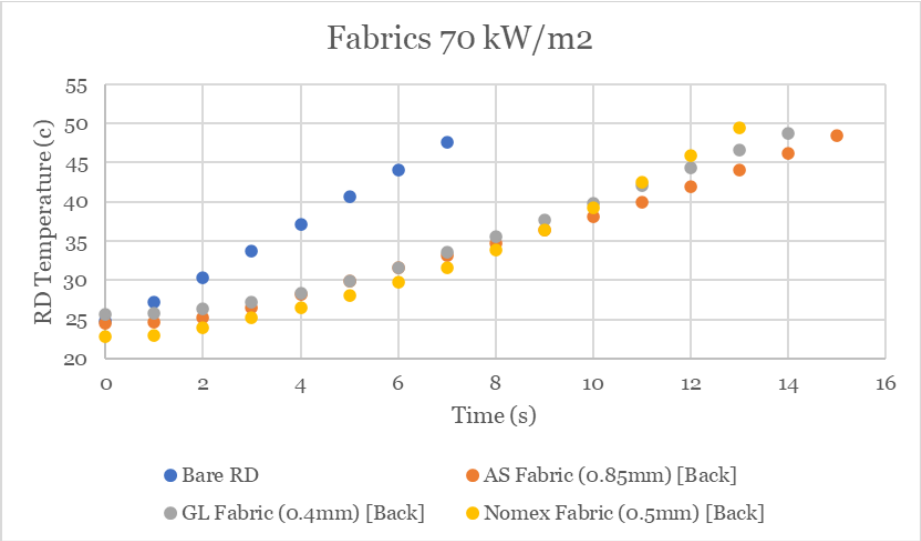

Figure 66: The combined data for the bare RD and the fabric tests at 70 kW/m².

Laminate 70 kW/m²

Two laminates were tested at 70 kW/m², the Nomex laminate and the AS fiberglass laminate. Based on the data collected, the Nomex laminate and the AS fiberglass laminate had equal performance. However, the Nomex laminate took more damage than the AS fiberglass laminate, and thus the AS fiberglass laminate can be determined to be the better material. While they came closer than the other tests, neither of these materials cleared the metric of 30 seconds under 70 kW/m². The results of these tests are included below.

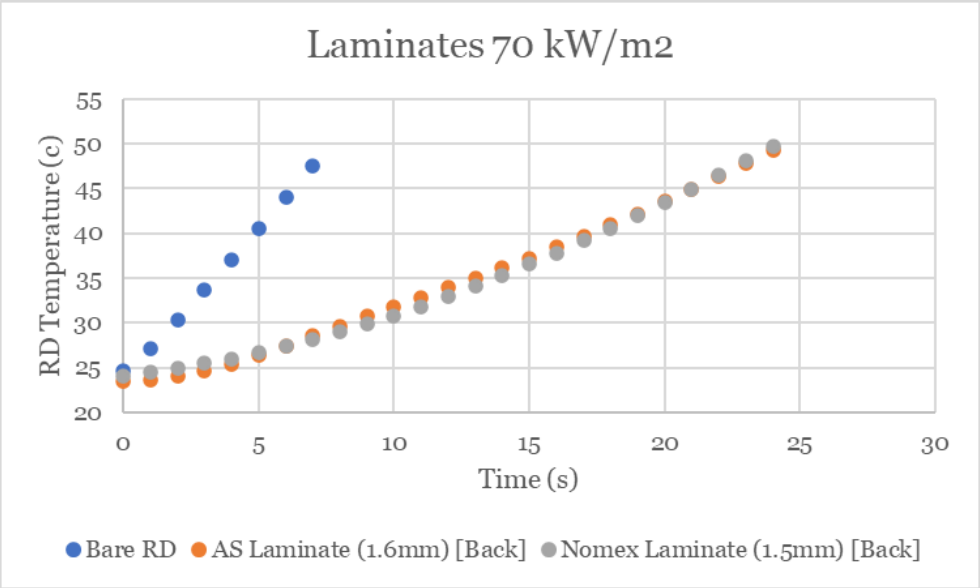

Figure 67: The combined data for the bare RD and the laminate tests at 70 kW/m².

PCM Back Orientation 70 kW/m²

The PCM back orientation was the only orientation considered for the comparison for the 70 kW/m² heat flux. This is because one test was performed at 70 kW/m² in the front orientation. Here for the assessment of the back orientation tests, we included the bare representative device, the AS fiberglass laminate, and the PCM and AS fiberglass laminate combined test. The PCM and laminate combination was the greatest performing of all the tests conducted at 70 kW/m². It was the only test to clear the metric of 30 seconds under a 70 kW/m² heat flux, and it cleared by that quite a large amount. Thus, this test was designated a success.

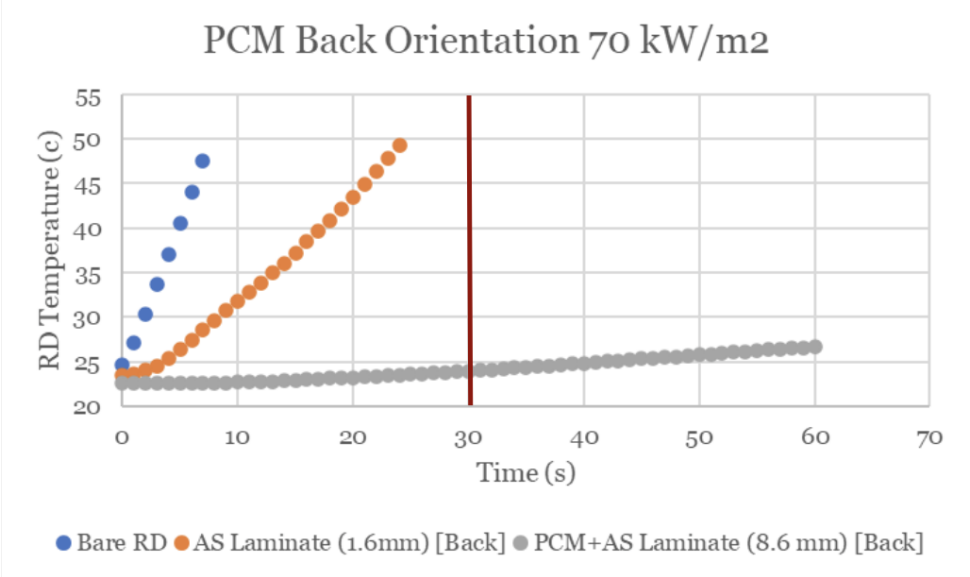

Figure 68: The combined data for the bare RD, the AS laminate, and the back orientation PCM tests at 70 kW/m². Highlighted in red is the success time for these tests.

All results 70 kW/m²

Of the 70 kW/m² tests, only one took longer than 30 seconds to reach 45°C. This was the PCM and Laminate combined test. It is important to consider when drawing comparison from this graph the difference made by different thicknesses of materials between the representative device and the heat flux.

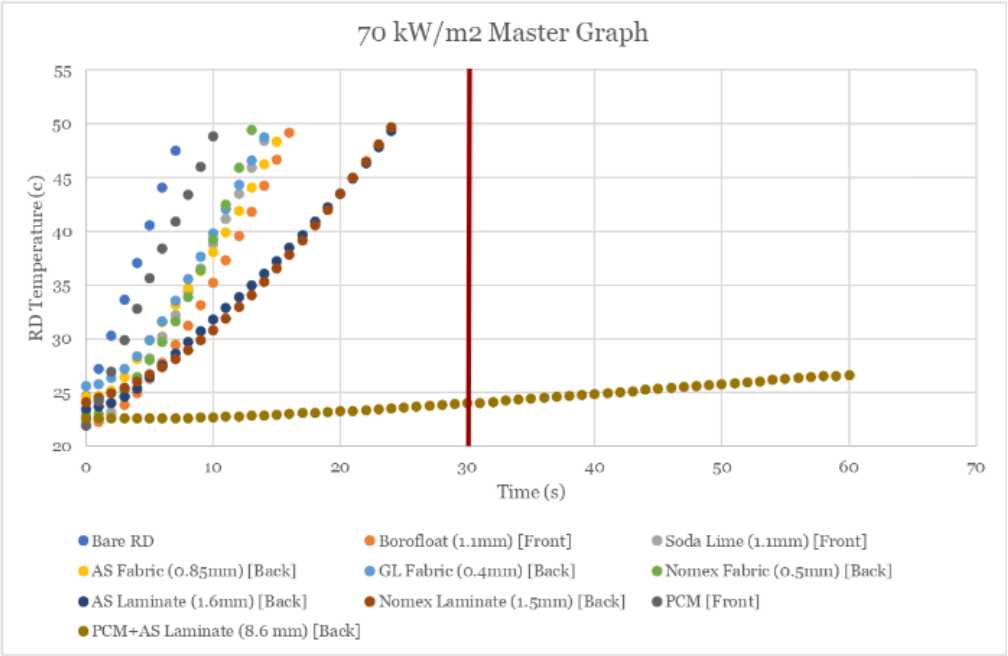

Figure 69: The combined data for all the tests conducted at 70 kW/m². Highlighted in red is the success time for these tests.

Glass Transmissivity Calculations

To predict certain necessary transmissivity values for the given thickness of glass determined to be 1.1 mm, the lumped capacitance approach can be implemented. This will allow the selection of time desired for the phone to last until 35 C, while being exposed under a certain flux, allowing one to determine the needed transmissivity of the glass substrate. The following expression was used:

$$\frac{dT}{dt} = \frac{q''_{ext}\tau - h(T - T_\infty) - 4\varepsilon T_{avg}^3 \sigma T}{\rho C_p \Delta x} X$$

Through integration:

$$\int dt = \int_{298}^{308} \frac{\rho C_{p\Delta x}}{q''_{ext}\tau - hT_\infty - \left(4\varepsilon\sigma T_{avg}^3 - h\right)T} dT$$

$$t = \left[\frac{\rho C_{p\Delta x}}{4\varepsilon\sigma T_{avg}^3 - h} \ln\left(\frac{q''_{ext}\tau - hT_\infty}{\rho C_{p\Delta x}} - \frac{4\varepsilon\sigma T_{avg}^3 - h}{\rho C_{p\Delta x}} T\right)\right] for\ 298K \rightarrow 308K$$

Using the following variables:

Table 8: Glass and RD properties (SCHOTT, Engineering Toolbox).

Property (units)	Value
ρ (kg/m^3)	2700
C_p $(kj/kg\ K)$	0.87
Δx (m)	0.00745
h $(kW/(m^2K)$	12
$\boldsymbol{\sigma}$ $(kW/(m^2K^4))$	$5.67 \cdot 10^{-11}$
T_{avg} (K)	303
T_∞ (K)	298

The following theoretical chart was created using the previous integration method. Each line corresponds to a certain heat flux, which remains constant. Various lower heat fluxes are given, including 5, 10 and 15 kW/m^2. In addition, our tested ranges were also included (20 and 70 kW/m^2).

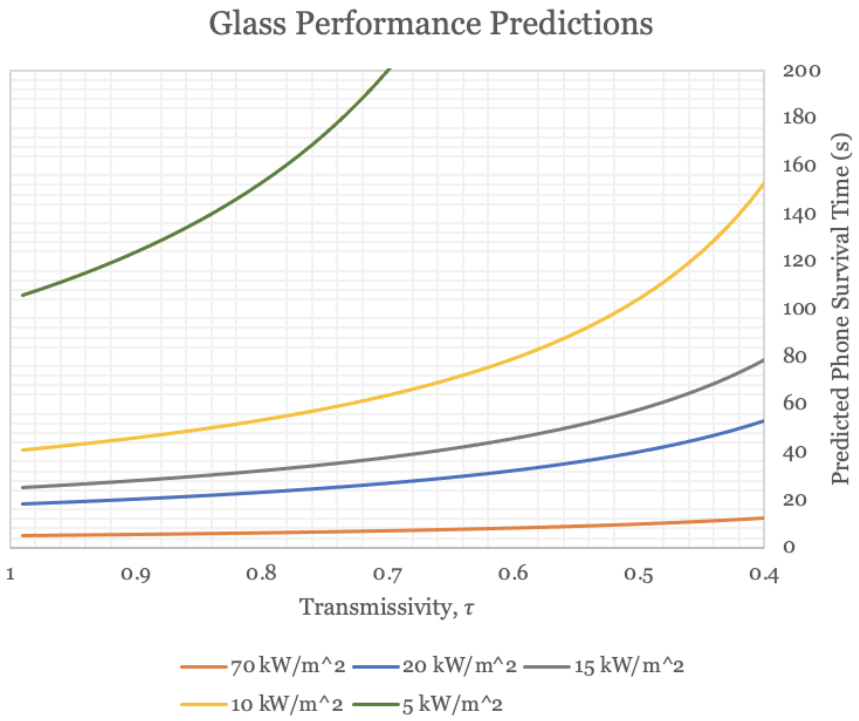

Figure 70: This chart shows the predicted time of phone survival when changing the transmissivity of the glass. Each line corresponds to a heat flux that is held constant.

The results of this analysis can show what sort of range of transmissivity glass could be selected for a desirable outcome. There is a tradeoff when selecting a glass with a lower transmissivity value. A decrease in transmittance, while decreasing the overall amount of radiation passing through the glass, will likely also decrease the amount of visible light passing through to the user. This is dependent on the specific makeup of the glass, and can vary depending on the transmissivity spectrum. In other words, the transmittance value will depend on the wavelength of light passing through.

Referring to the results discussed earlier, we can determine which transmissivity would provide sufficient protection for the RD to survive the conditions laid out in Table 4. From the analysis done on this system at 20 kW/m^2, the transmissivity would have to be extremely low for the glass to come close to meeting the condition of 60 seconds. At lower fluxes, such as 5 and 10 kW/m^2, the RD would still be able to survive for extended periods of time with reasonably high transmissivity values. For example, Figure 70 shows that under 5 kW/m^2, a transmissivity of 0.8 would yield a predicted survival time of over 150 seconds. It also indicates that a transmissivity of 0.73 could potentially increase the survival time beyond 60 seconds under 10 kW/m^2. These lower transmissivities could have a negative impact on optical qualities, and this could be examined more. It is important to note that while these tests indicate "survival time," the RD does still maintain function until 45^{o}C. This same simulation could be completed with a range from 25^{o}C to 45^{o}C.

Follow-up Screen Protector Study

The follow-up study performed during D-term tested the six materials purchased with the goal of finding a more ideal screen protector material. The first material tested was the high temperature quartz glass. This material was a 2.5in glass square with a thickness of 1/16" (1.5875 mm). This material was too thick for the touch screen to work, but was the thinnest quartz material available. Because of this, we opted to test with it anyways. The BG38 NIR Cut 2 optical filter was the next material. It was a 2 in square, and was 1 mm thick. The NG5, NG11, KG2, and KG5 were all 1-inch diameter circles with a thickness of 1 mm. The new representative device was also tested on its own. The results of this testing can be seen in Figure 71 below.

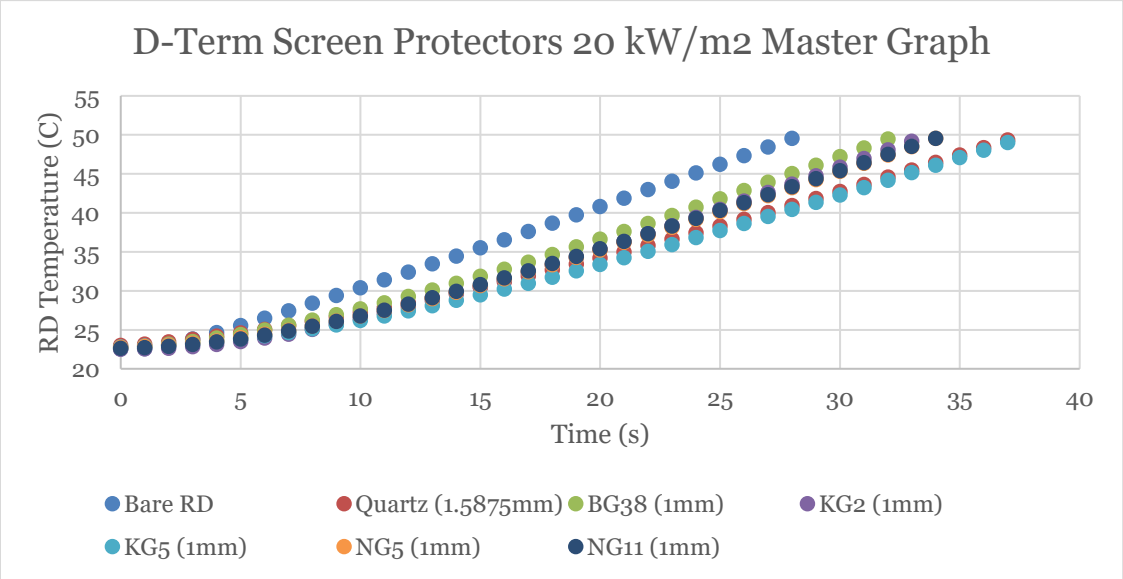

Figure 71: The results from the D-term follow-up study.

In addition, the results of the screen protector materials tested in the main project were also included in the following figure below.

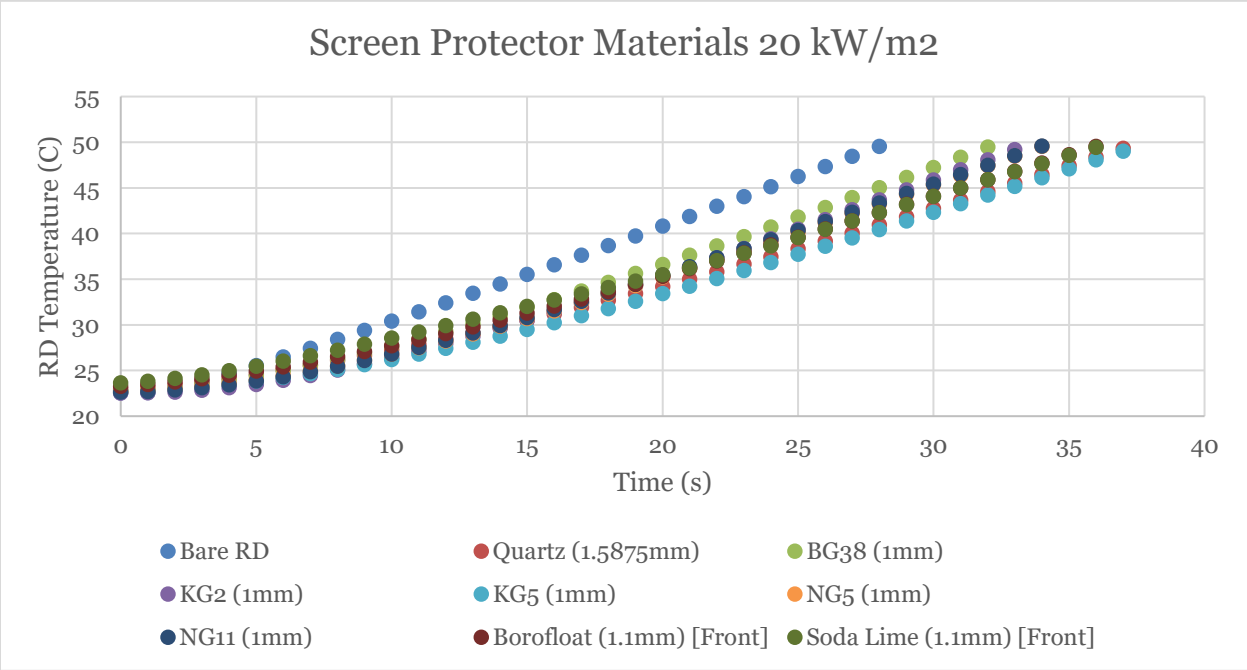

Figure 72: The results of testing all screen protector materials, both during the main and follow-up study.

The screen protector materials tested during the follow-up study saw little improvement in performance compared to the screen protector materials tested during the main project. While the range of results suggests that internal transmittance does have some effect on the results of this testing The KG5 Schott optical filter had the best performance of all these materials tested. It took 38% longer for the representative device with the KG5 to reach 45°C than the bare representative device, whereas the Borofloat and soda lime glass saw a 29% increase in performance over the bare RD at 20 kW/m².

Conclusions and Recommendations

Conclusions

Through the testing of the chosen materials at both 20 kW/m² and 70 kW/m², we have found that significant measures are required in order to shield a phone from the heat flux of a fire environment. These two testing conditions are rigorous, and subject the materials to extreme conditions. To reiterate, the typical amount of time which the average firefighter can tolerate in 10 kW/m² is only one minute. This means that any configuration which passed even our lower flux test of 20 kW/m² has proved to be very effective. When testing with a heat flux of 20 kW/m², both the back orientation PCM and the back orientation PCM and AS fiberglass laminate combination can be considered successes. For the 70 kW/m² tests, only the PCM and AS fiberglass laminate combination achieved the 30 second metric for success. The PCM and Laminate combination test was the only one able to pass both the 20 kW/m² and the 70 kW/m² metrics.

These layers combined have shown considerably more protection than any single protection layer on its own. The thermal degradation for the PCM and laminate combination has proved to also be very minimal under pre-flashover conditions. Even in extreme flashover conditions, the proposed casing apparatus had surpassed the defined conditions for success. With respect to the glass, the resistance to heat flux has shown promise in the lower heat flux simulation. Specifically, the 5 and 10 kW/m^2 simulation results showed that the glass of slightly lower transmissivity could potentially yield very long survival times for the RD.

For 20 kW/m^2, the following performances were measured. On average the glass materials performed 29% better than the bare representative device. The fabrics performed, on average, 46% better than the bare representative device. The laminates performed approximately 125% better than the bare representative device. The phase change material in the back position performed 246% better than the bare representative device. Finally, the phase change material and the laminate together performed 733% better than the bare representative device. For 70 kW/m^2, the following performances were measured. The glasses and fabrics both performed approximately 86% better than the bare representative device. The laminate performed 200% better than the representative device. Finally, the phase change material and laminate combination performed at least 750% better than the bare representative device. Because that test was ended early, the actual percent increase in performance is indeterminate. Finally, the highest performing of the screen protector materials tested in D-term, the KG5, performed 38% better than the bare representative device.

Recommendations

To improve the effectiveness of the glass and casing apparatus, we have suggested some alternative solutions. The first recommendation following this project is to examine other phase change material options. The primary one that we would recommend further investigating is hydrated salts. While we elected not to test with hydrated salts in this project, this was due to lack of literature support. The flammability of the paraffin wax makes this a hazardous material for the purposes at hand, so non-flammable hydrated salts would be a good option for investigation. The second recommendation we would make following this project would be to refine the laminate. While the laminate we fabricated was suitable for our purposes, our observations throughout this project suggest that it could be improved. It would be worthwhile to try different curing methods for the laminate and mixing the pyro-paint with a thinner that would act as a solvent and improve the impregnation of the fabric. Additionally, it would also be worthwhile to investigate professionally made laminates that might be able to serve this purpose. Finally, use of a properly developed heat sink, rather than the thermal pathing that we made, would likely improve the performance of the phase change material, and should be investigated further.

For the glass, there are several potential routes which could be researched further. As stated previously, the glass screen protector can have a maximum thickness of 1.1 mm, meaning that adding any additional glass would render the capacitive touch screen unusable. This means that the properties of the glass must be different, or no glass can be used for heat resistant screen protection under these conditions. It is an option to use a layered laminate and PCM setup like

our casing to cover the screen, although this too would leave the screen unusable. There are a few options that could be pursued for the glass screen protector.

1. The use of a 1-way reflective coating, which could provide additional heat protection against radiation.
2. The use of an actuated tinting mechanism, like electronic welding lenses, that can change optical transmissivity through some sort of stimuli, usually electronic.
3. The use of a fused quartz material as a screen protector. This was going to be tested alongside the borosilicate and soda lime glasses in this project. However, due to supply shortages, this was not possible as the waiting times for substrates of our desired dimensions were far too long.

Overall, the screen has presented a challenge due to its requirement of a small thickness compared to the case, but there are still possible resolutions which we did not investigate during this project.

Appendix A: Fourier Number Determination for Lumped Capacitance

Fourier's number was found with the following system to assess the validity of the use of lumped capacitance:

$$Fo = \frac{\alpha \cdot t}{(\Delta x)^2}$$

Using the thermal resistance network method, each layer's thermal resistance was calculated using their thickness, thermal conductivity, and the cross-sectional area:

$$R = \frac{\Delta x}{k \cdot A}$$

Table 9: Thermal conductivities of constituent layers and their corresponding thermal resistances. The total heat capacity was found using a weighted average of the individual heat capacities using the volume percent of each layer. The total thermal conductivity was found by rearranging the previous equation and using parameters for the system. The overall density was found by using the total mass divided by the total volume (SCHOTT, Rubitherm Technologies, Architectural Fiberglass, Engineering Toolbox).

Property	Glass	Phone (aluminum)	PCM	Fiberglass Laminate	Total
ρ (kg/m^3)	2200	2700	880	2500	1777.8
$C\ (J/\ kg\ K)$	830	900	2000	790	1397.8
$\Delta x\ (m)$	0.0011	0.00635	0.01	0.00368	0.02113
$A_s\ (m^2)$	0.00403	0.00403	0.00403	0.00403	0.00403
$V\ (m^3)$	0.00000443	0.00002559	0.0000403	0.00001483	0.000085
$m\ (kg)$	0.0097526	0.06909435	0.035464	0.037076	0.1514
$k\ (W/\ m\ K)$	1.12	100	0.2	0.05	0.17
$R\ (W/\ K)$	0.244	0.016	12.41	18.26	30.93

With these parameters, the diffusivity, α , was found for the entire system where:

$$\alpha = \frac{k}{C \cdot \rho}$$

Diffusivity, $\alpha = 6.821 \times 10^{-8}\ m^2/s$

Using the previously given equation for Fourier's number and at a time of 120 seconds:

$$Fo = 0.0183$$

This means the lumped capacitance method could prove to be somewhat inconsistent with our system as there is a reasonable presence of a thermal gradient.

Appendix B: Suitability of Aluminum as Representative Device (RD)

Using parameters in table 10 below, obtained through literature on smartphone components:

Table 10: Parameters for smartphone components used to verify the representative device feasibility. The table was sourced from Kim et al.

Component	Thickness (m)	Area (m^2)	Volume (m^2)	Volume %	Heat Capacity (*10^6 J/m^3 K)
Glass	0.001	0.011343	0.000011343	0.1123595506	1.83
Backplate	0.00025	0.011343	0.00000283575	0.02808988764	1.35
Graphite sheet	0.000025	0.011343	0.000000283575	0.002808988764	1.52
PCB	0.0008	0.011343	0.0000090744	0.08988764045	1.332
Shields	0.00015	0.011343	0.00000170145	0.01685393258	3.64
Metal bracket	0.000275	0.011343	0.000003119325	0.03089887764	3.64
Display lumped	0.002	0.011343	0.000022686	0.2247191011	1.2
Heat pipe	0.0004	0.011343	0.0000045372	0.04494382022	3.4944
Battery	0.004	0.011343	0.000045372	0.4494382022	2.193

With thickness and area, these dimensions were used to calculate volume of each component (Kim et al.). These individual volumes were compiled into a total volume, and then each component volume was taken as a percent of the entire phone system volume. With this information and the given heat capacities, a weighted average was taken to determine the device's theoretical total heat capacity, C_P. It was determined that $C_P = 1.95 * 10^6 J/m^3K$

Using a heat capacity for aluminum of 900 J/m^3K, and a density of aluminum of 2700 kg/m^3, the heat capacity of the aluminum in the desired units was found to be $C_P = 2.43 * 10^6\ J/m^3K$. Considering that a slab of aluminum of similar thickness to a smartphone has a reasonably consistent heat capacity, it was deemed that this representative device was suitable for our testing.

Appendix C: Fabrication of Laminates

Each of the fabrics, including Nomex and the Fiberglass, were cut into squares measuring 2.5" x 2.5." These squares were cut using shears. Any remaining frayed fibers were cut off as well. These squares were coated with a liberal amount of PyroPaint on both sides and allowed time to soak. This was done using a foam paint brush. After sufficient soaking, the soaked fabrics were coated once again. Each square was allowed to dry over the course of several days in between lab testing sessions. Initially, the laminates were hung using a wire as seen below.

Figure 73: Initial coatings on the laminates were allowed to dry shown above. Nomex pictured on the left and the AS Fiberglass on the right.

Upon finding this single coating still yielded a flexible laminate, both fabrics were allowed to soak again and dry. After speaking with Aremco regarding the curing process, a grated wire drying rack was used to lay each laminate dry. A total of three coatings were applied to the laminate. Like the previous method, a dish was to be formed using laminated fabric so as to catch any PCM which drips below the sample. Initial tests were performed to see how much, if any, melted PCM would absorb into the laminate.

Using our previously formed laminate of AS Fiberglass and PyroPaint, a small amount of melted PCM was placed on the corner and allowed time to absorb. The mass of the Laminate was taken prior to PCM absorption testing. The mass was then taken to determine precisely how much PCM was used, and then after scraping off as much as possible without damage to the laminate, the mass of the system was taken one final time. It was determined that 70% of the PCM was able to be removed, meaning the remaining 30% absorbed into the laminate.

Regardless of this test, we still needed a rigid dish to collect melted PCM, so the fabrication continued. A spare aluminum square, nearly identical to our RD, was used as a mold to fabricate this dish. After soaking in PyroPaint, zip ties were used to secure the soon-to-be laminate to the aluminum square, giving us a dish that was the desired size. This was allowed to cure and 2 more coatings were applied like our tested laminates

Although we did obtain reasonable performance from our laminates, they could be improved, in rigidity, homogeneity, and durability. Possible flaws in our laminates could be caused by insufficient curing, as well as insufficient impregnation of the fabrics with the PyroPaint. By experimenting with various curing cycles, both in air and under heat, the optimal curing for the laminates could be determined. Similarly, by using a compatible solvent as a thinner, the PyroPaint could be allowed to absorb more thoroughly into the fabric surface, possibly allowing for a better cure and a more durable final product. Due to time constraints, we only used one method of fabrication for our laminates.

Appendix D: Construction of PCM Apparatus

Prior to Fabricating our PCM block, we needed to construct the thermal pathing network. The concept is simple: a bottom plate with short perpendicular fins along the surface to help dissipate heat. This was attempted first by using only stainless-steel mesh, but the shorter fins proved to be extremely flimsy and unusable. Instead, we opted for the same stainless steel bottom plate (measuring 2.4” x 2.4”), and aluminum mesh fins, which were much more rigid. These fins were spot welded to the baseplate as seen below alongside the finished product.

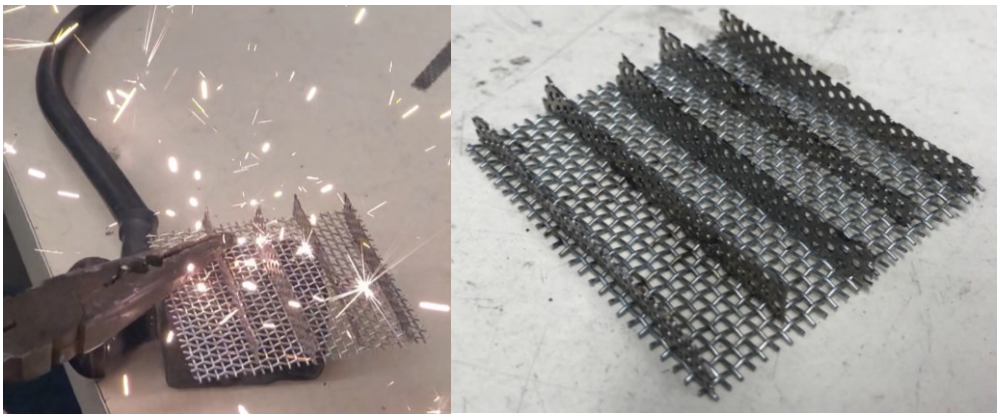

Figure 74: These two images taken in the lab show the spot welding of the fins (left) and the finished thermal pathing network (right).

With the thermal pathing assembled, the rest of the PCM layout needed to be created. The bulk PCM was received in solid form (a large block inside a bottle). In order to remove PCM, a pick tool was used to break off chunks of PCM. These smaller chunks were placed into a Ziplock bag and further ground up, yielding a fine powder.
Prior to the melting of PCM, a fitted mold was made by surrounding the RD with aluminum foil. This would allow the PCM to adhere to the back face of the RD. The thermal pathing was added on the back of the RD before pouring.

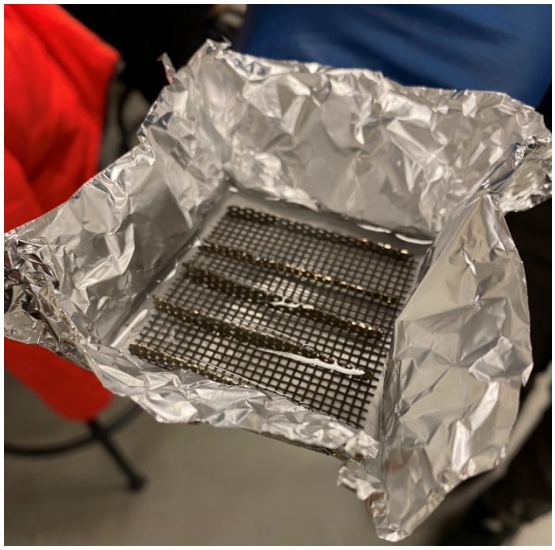

Figure 75: This image shows the aluminum mold that was used to contain the liquid PCM when forming. The PCM sits on the back face of the phone where the thermal pathing is submerged.

The liquid PCM was poured until the thermal pathing was submerged. This was left to dry in the freezer for about 20 minutes.

Figure 76: This image shows the PCM when fully solidified. The solid PCM surrounds the thermal pathing, and the RD sits underneath it.

As described previously, the PCM needed to be contained when melted during testing, so a fiberglass laminate dish was fabricated. This can be recalled from Appendix C. The dish was finally covered in aluminum foil, and the dish would sit underneath the configuration when testing.

Appendix E: Budgets

Table 5: Budget for this project. Deviations from the budget established in early B-term will be explained.

Item	Supplier	Quantity	Unit Price ($)	Total ($)	Cost Notes
AMI-Glas (GL) (black)	Auburn Manufacturing	3 x (8”x10”)	8	24	
AMI-SIL (AS)	Auburn Manufacturing	3 x (8”x10”)	8	24	
PyroPaint 634-AS1	Aremco	1 Pint	100	100	Much more reasonable quantity than Accumet + cheaper price
Nomex iiiA	Westex: Milliken	36” x 36”	FREE	FREE	Quoted $300 from other suppliers for similar quantity
Fused Silica	Abrisa Technologies	2 x fused silica	150	300	Seller has a $300 minimum, getting two allows us some room in case one breaks
Soda lime	S.I Howard Glass	10	Free	Free	Free samples given upon request from sales
Borofloat	Cincinnati Gasket	10	5.25	52.50	Half the unit cost of Borofloat compared to Abrasia
Screen protectors	Dollar Store	6	5.55	33.3	Lowest cost protectors we could find

Aluminum Chunk	WPI welding lab	1	FREE	FREE	Found in scrap and cut to size
RT 35 HC	Rubitherm	1 kg	€14.70/kg	€119.60 (shipping and other fees included) ($120.35)	Euro prices will fluctuate slightly compared to dollar prices
Total Cost				$654.15	
Contingency		20%	$667.15*0.2	$130.83	In case something goes wrong
Total Cost + contingency				$784.98	

Each material listed here was here for a reason. The aluminum that was chosen to be the representative device used as a standin for the phone. This was deemed a suitable replacement for a phone in our testing based on the heat capacity analysis performed in the materials and design section and in appendix B. Additionally, it was free and thus was a great choice for the representative device. The screen protectors that are included in the budget above were bought to test the maximum thickness that could be used and still allow the screen to function.

The RT 35 HC is a paraffin wax phase change material ordered from Rubitherm technologies, a German company. This material was chosen because it has a high heat of fusion and an ideal melting point. This makes it an ideal material for absorbing heat that would enter the phone. The Borofloat was the first screen protector material that we wanted to test. Very few high temperatures glass materials are both clear and manufactured at a thin enough thickness to still allow for the screen to work. The Borofloat is a borosilicate glass that meets these material parameters. This made it an ideal material for testing. The other screen protector material that we were initially going to test was the fused silica. While the supplier initially said that they had this material, when we attempted to order it, we were informed that there was a national shortage of fused silica, and their inventory will be sold out until 2024. Because of this, this material will not be able to be tested in this project. Instead, we opted to test a soda-lime glass instead. While this glass does not have the high temperature properties that the fused silica has, it does allow us to get a basis for comparison to see whether the Borofloat makes a significant difference to the heat that reaches the representative device compared to ordinary glass. Soda-lime glass was provided to us for our testing by S.I Howard Glass free of charge.

Three materials were considered for the laminate. The first was the AMI-Glas (GL) (black). This material was chosen for its heat resistant properties. The second was the AMI-SIL (AS),

which was chosen for the same reason. We were able to get sample pricing from Auburn Manufacturing, the supplier for this material. The third material for the laminate was the Nomex iiiA. For this material, we were able to get a free sample from the supplier, Westex: Milliken. Finally, one adhesive was bought for making the laminate, the PyroPaint 634-AS1. This is a high temperature ceramic adhesive, making it suitable for making a laminate that can withstand high temperatures.

Table 6: Follow-up study budget for this project.

Item	Supplier	Quantity	Unit Price ($)	Total ($)	Cost Notes
Quartz glass 2.5in square	McMaster	1	33.93	33.93	
Schott KG5 25mm diameter	Edmund Optics	1	34	34	1 inch square not available, 1 inch circle much cheaper than 2-inch square
Schott KG2 25mm diameter	Edmund Optics	1	34	34	1 inch square not available, 1 inch circle much cheaper than 2-inch square
Schott BG38 50mm square	Edmund Optics	1	88	88	Only other size is half inch diameter square
Schott NG5 25mm diameter	Edmund Optics	1	39	39	1 inch square not available, 1 inch circle much cheaper than 2-inch square
Schott NG11 25mm diameter	Edmund Optics	1	39	39	1 inch square not available, 1 inch circle much cheaper than 2-inch square
Total Cost				267.93	
Contingency				15%	For shipping or price fluctuation
Total + Contingency				308.12	

References

Abecassis Empis, C. (2010). Analysis of the compartment fire parameters influencing the heat flux incident on the structural façade.

Architectural Fiberglass, I. (n.d.). *Fiberglass (FRP) properties*. Architectural Fiberglass, Inc. - Fiberglass Properties.

Barker, J., Boorady, L. M., Lee, Y. A., Lin, S. H., Cho, E., & Ashdown, S. P. (2013). Exploration of firefighter turnout gear part 1: identifying male firefighter user needs. *Journal of Textile and Apparel, Technology and Management*, *8*(1).

Bartholmai, M., Schriever, R., & Schartel, B. (2003). Influence of external heat flux and coating thickness on the thermal insulation properties of two different intumescent coatings using cone calorimeter and numerical analysis. *Fire and materials*, *27*(4), 151-162

Bergman, T. L., Lavine, A. S., Incropera, F. P., & DeWitt, D. P. (2011). *Introduction to heat transfer*. John Wiley & Sons

Carvill, J. (1994). *Mechanical engineer's data handbook*. Butterworth-Heinemann

Corning. (n.d.). Corning Pyroceram: Glass-ceramic material. Corning.

Custom Glass Fabrication & Optical Coatings. Abrisa Technologies. (2022, November 10)

Donnelly, M. K., Davis, W. D., Lawson, J. R., & Selepak, M. J. (2006). *Thermal environment for electronic equipment used by first responders*. National Institute of Standards and Technology. Building and Fire Research Laboratory.

Engineering ToolBox. (n.d.). *Metals - specific heats*. Engineering ToolBox.

Foster, J. A. and Roberts, G.V., "Measurements of the Firefighting Environment – Summary Report," Central Fire Brigades Advisory Council Research Report number 61, 1994, Home Office Fire Research and Development Group, Fire Engineers Journal, United Kingdom, September 1995.

Heat resistant cloth and fabrics for high heat MRO applications. Auburn Manufacturing, Inc. (n.d.).

If your iPhone, iPad, or iPod touch gets too hot or too cold - Apple Support. (2021, December 16). Apple Support.

Industrial Glass, window & gasket manufacturer. Cincinnati Industrial Glass. (2020, June 30).

Interactive filter diagram. SCHOTT. (n.d.).

Kim, K. M., Jeong, Y. S., & Bang, I. C. (2019). Thermal analysis of lithium ion battery-equipped smartphone explosions. *Engineering Science and Technology, an International Journal*, *22*(2), 610-617.

McCarthy, L. K., & Di Marzo, M. (2012). The application of phase change material in fire fighter protective clothing. *Fire Technology*, *48*(4), 841-864.

Metals and alloys - densities. Engineering ToolBox. (n.d.). Retrieved December 16, 2022, from https://www.engineeringtoolbox.com/metal-alloys-densities-d_50.html

National Fire Protection Association, NFPA 1971 Standard on Protective Ensemble for Structural Fire Fighting, 2000 Edition, Volume 11. National Fire Protection Association, 1 Batterymarch Park, P.O. Box 9101, Quincy, MA 02269-9101.

National Institute of Standards and Technology (NIST) federal building and fire safety investigation of the world trade center disaster answers to frequently asked questions (August 30, 2006). NIST. (2016, September 21).

Phase Change Material (PCM) Selection | PCM Technology. (n.d.). Phase Change Material (PCM) Selection | PCM Technology.

Phelps, H., Sidhu, H. (2015). A mathematical model for heat transfer in fire fighting suits containing phase change materials. Fire Safety Journal, 74, 43–47.

Rubitherm Technologies. (n.d.). *Data sheet - rubitherm*. Data Sheet: RT 35 HC.

SCHOTT. (n.d.). Schott Borofloat® technical details. SCHOTT.

ScienceDirect. (n.d.). Compartment fire. Compartment Fire - an overview | ScienceDirect Topics.

Soda-lime glass material properties. Imetra, Inc. (2020, June 10).

Standard test method for radiant heat resistance of flame resistant clothing materials with continuous heating. ASTM International - Standards Worldwide. (n.d.). Retrieved December 17, 2022

Technical properties of NEXTREMA® heat-resistant glass. SCHOTT. (n.d.). Retrieved October 13, 2022

Touch Sensor Front Panel: How to choose the right cover glass. Fieldscale. (2021, March 5). Retrieved October 13, 2022

Venkatapathy, E. (2019, October). Ablators-From Apollo to Future Missions to Moon, Mars and Beyond. In *International Astronautical Congress* (No. ARC-E-DAA-TN74395).